MELCHIOR, P.
Observatoire Royal de Belqique
Bruxelles
Belgium

Proc.Symposium on Earth's Gravitational Field & Secular Variations in Position (1973),509-521.

ON EARTH TIDE MODELS FOR THE REDUCTION OF HIGH PRECISION QUASI-RADIAL RANGE MEASUREMENTS

ABSTRACT

The problem of the Earth's deformation is one of spherical elasticity of the sixth order. The importance of Earth tides in astronomy and geophysics is emphasised by their relation to the precession-nutation and tesseral tide problems, the secular retardation of the Earth's rate of rotation due to the dissipation of energy in sectorial tides, the periodic variations in the rate of rotation due to zonal tides, satellite orbit perturbations due to variations in the Earth's potential, and the radial deformations in laser distance measurements.

The possibility that dynamical effects would be produced in the Earth's liquid core was pointed out by Poincare, and developed by Jeffreys, Vicente and Molodensky. An experimental confirmation is presented. The role of the Earth tide phenomenon in geodetic space research is also described, along with perturbing effects due to regional tectonic features. Instrumental developments are critical in the acquisition of precise data; the calibration problem is fundamental for a correct comparison with Earth models and the reduction of quasi-radial range measurements.

1. Text

We are concerned during this Symposium with the possibility of correcting the Earth-Moon or Earth-satellites distance measurements from the effects of tidal deformations with a precision of 1 cm.

The Earth-Tide theory as well as the observations use the well known Love numbers for a representation of all types of solid-Earth deformations.

The main difficulty in the interpretation of Earth tide observations in terms of these Love parameters is due to the indirect effects of the oceanic tides.

This very clearly appears in clinometric measurements, in satellite orbit perturbations and at a lower degree (but in any case not negligible) in gravimetric measurements.

The deformation component needed for correcting the laser distance measurements to the Moon and satellites is obviously the radial displacement. Unfortunately it cannot be measured directly with geodynamical instruments. The classical way to derive it consists of a combination of tidal gravity and tidal tilt measurements which respectively give the amplitude ratios to a rigid Earth described by the coefficients

$$\delta = 1 + h - \frac{3}{2} k \qquad (1)$$

and

$$\gamma = 1 + k - h \qquad (2).$$

Then

$$k = 4 - 2(\gamma + \delta) \qquad (3)$$

and

$$h = 5 - 3\gamma - 2\delta \qquad (4).$$

h is the elastic parameter of interest as it characterizes the static radial deformation

$$\xi = h \frac{W}{g} \quad ,$$

W being the tidal potential.

However it is not permissible to derive h as given by equation 4 if the observed quantitites γ, and δ are disturbed by important regional superficial effects like ocean loading, oceanic attraction and also thermic or barometric perturbations.

Thermic and barometric perturbations strongly affect the clinometric measurements but they can be eliminated fairly well if sufficiently deep stations (minimum 50 m depth) are installed and if periods of observations of a minimum of one year are available.

The problem of investigating and eliminating the ocean loading and the consequent change of potential and attraction, is quite different. There are three ways of progressing in that difficult question:

(a) By making observations with good and well calibrated instruments in the very centre of continents and from there, develop trans-continental profiles. Such profiles are now observed in the United States (by Kuo), Europe (by Melchior and Kuo, Honkasalo, Bonatz, Stuckenbroker, and others) and Asia (by Melchior and Ducarme).

(b) By making a computation of the ocean loading effects on the basis of a model of the crust constitution and a precise cotidal chart. This procedure is developed by J.T. Kuo, W. Farrel, D. Bower and B. Pertsev.

(c) By concentrating our attention not on the semi-diurnal components but on the diurnal ones. The diurnal tides have, by chance, very little amplitudes in the main oceans.

Indeed, it can be observed from table 1 that the γ factor which is extremely sensitive to oceanic indirect effects, remains very homogeneous and stable all across Europe for each of the three main diurnal components although the oceanic tides have important amplitudes and a very complicated distribution around the European coasts. But their diurnal components are always of very small amplitude. Therefore let us consider, as a first step, the results obtained for the diurnal waves. These waves are of primary importance in astronomy and geophysics: they are tesseral waves and are produced by the same part of the tidal potential as the astronomical precession and nutation (MELCHIOR 1973, volume 4).

For example:

K_1 wave is associated with the precession;
P_1 wave is associated with the semi-annual nutation; and
O_1 wave is associated with the fornightly nutation.

As they are of tesseral nature, liquid core dynamical effects can modify their amplitudes by resonance as demonstrated by Poincaré. This effect has been calculated for several Earth models by Jeffreys & Vicente, and by Molodensky.

The O_1 wave frequency, being far from the resonance frequency, can be considered as representing the pure static deformation.

As the O_1 wave has a period of $25^h\ 49^m$, it is out of the strong diurnal noise of 24 hour period and

Table 1

Dynamical Effects of the Earth's Liquid Core on the Tesseral Diurnal Waves

A. CLINOMETRIC MEASUREMENTS - HORIZONTAL EW COMPONENT.

	N	AMPLITUDE FACTORS K1	P1	O1	Q1	PHASE K1	P1	O1	Q1	INSTR
BELGIUM										
SCLAIGN.1 EW	2512	0.7519	0.697	0.6825	0.656	7.31	13.59	10.54	16.35	VM 1
SCLAIGN.1 EW	2512	0.0058	0.018	0.0081	0.042	0.44	1.48	0.68	3.66	VM 31
SCLAIGN.2 EW	544	0.7269	0.654	0.6883	0.730	8.82	13.56	8.82	11.70	VM 67
SCLAIGN.2 EW	544	0.0153	0.049	0.0203	0.103	1.21	4.34	1.69	8.10	VM 67
SCLAIGN.3 EW	1718	0.7697	0.740	0.6879	0.834	8.31	13.34	7.35	12.86	VM 55
SCLAIGN.3 EW	1718	0.0072	0.023	0.0098	0.051	0.53	1.80	0.81	3.48	VM 55
DOURBES 1 EW	3062	0.7544	0.724	0.6671	0.637	-2.24	-3.93	0.29	1.45	VM 8
DOURBES 1 EW	3062	0.0028	0.009	0.0039	0.020	0.22	0.73	0.33	1.81	VM 8
DOURBES 2 EW	2924	0.7545	0.725	0.6670	0.571	2.61	3.93	8.76	6.44	VM 28
DOURBES 2 EW	2924	0.0031	0.010	0.0042	0.022	0.23	0.80	0.36	2.21	VM 28
KANNE EW	1678	0.7520	0.688	0.7186	0.629	-7.85	-3.34	-14.49	-11.37	VM 72
KANNE EW	1678	0.0086	0.029	0.0117	0.061	0.66	2.41	0.93	5.55	VM 72
LUXEMBURG										
LUXEMBG. EW	410			0.6458				-5.39		VM 65
LUXEMBG. EW	410			0.0418				5.79		VM 65
WALFERD.1 EW	1176	0.7591	0.737	0.6816	0.637	-3.09	-1.38	0.88	-3.37	VM 42
WALFERD.1 EW	1176	0.0042	0.014	0.0057	0.030	0.33	1.11	0.49	2.75	VM 42
WALFERD.2 EW	870	0.7553	0.728	0.6395	0.602	-5.13	-7.34	-4.09	5.53	VM 42
WALFERD.2 EW	870	0.0058	0.019	0.0078	0.040	0.44	1.50	0.71	3.88	VM 12
WALFERD.3 EW	320	0.7338	0.764	0.6727	0.590	-4.21	-2.91	-7.60	-17.72	TSB 16
WALFERD.3 EW	320	0.0178	0.057	0.0241	0.121	1.40	4.26	2.05	11.79	TSB 16
CZECHOSLOVAKIA										
PRIBRBL. EW	846	0.7321	0.622	0.6917	0.693	-14.87	-19.22	-15.29	-21.97	VM 77
PRIBRBL. EW	846	0.0084	0.028	0.0112	0.058	0.65	2.59	0.93	4.83	VM 77
GERMANY										
BAD GRUND EW	312	0.7554	0.687	0.6787	0.636	6.79	5.39	11.75	14.90	VM 64
BAD GRUND EW	312	0.0082	0.027	0.0111	0.058	0.64	2.37	0.97	5.38	VM 64
TIEFEN. EW	1048	0.7330	0.793	0.6745	0.634	2.42	3.85	3.10	1.37	SW
TIEFEN. EW	1048	0.0098	0.028	0.0141	0.072	0.20	0.57	0.29	1.48	SW
AUSTRIA										
GRAZ EW	598	0.7359	0.826	0.6476	0.603	15.40	18.13	19.62	31.60	VM 44
GRAZ EW	598	0.0123	0.040	0.0166	0.087	0.96	2.80	1.47	8.30	VM 44
HUNGARY										
SOPRON EW	91	0.7558		0.6965	0.664	-1.40		5.27	2.94	VM 44
SOPRON EW	91	0.0122		0.0188	0.104	0.97		1.55	8.86	VM 44
SWEDEN										
DANNEM. EW	2954	0.7353	0.680	0.7100	0.712	-5.02	-8.09	-0.47	5.73	VM 38
DANNEM. EW	2954	0.0039	0.013	0.0054	0.027	0.31	1.09	0.43	2.21	VM 38
FINLAND										
LOHJA EW	780	0.7163	0.616	0.6983	0.716	0.35	7.56	2.83	3.68	VM 89
LOHJA EW	780	0.0085	0.029	0.0112	0.059	0.68	2.69	0.92	6.07	VM 89

VM VERBAANDERT - MELCHIOR QUARTZ PENDULUM
SW SCHWEYDAR PENDULUM
TSB TSUBOKWA ELECTROMAGNETIC PENDULUM

T a b l e 1 (Continued)

Dynamical Effects of the Earth's Liquid Core on the Tesseral Diurnal Waves

B. GRAVIMETRIC MEASUREMENTS - VERTICAL COMPONENT
****

RECENT TIDAL GRAVITY PROFILES /PROVISIONNAL RESULTS/
****

			FACT.AMPLITUDE				PHASE				INSTR
		N	K1	P1	O1	Q1	K1	P1	O1	Q1	
FUNDAMENTAL STATION FOR CALIBRATION											
BRUXELLES	V	606	1.1505	1.164	1.1641	1.176	0.23	-0.23	-0.01	-0.32	G 84
BRUXELLES	V	606	0.0017	0.005	0.0023	0.011	0.08	0.26	0.11	0.56	G 84
BRUXELLES	V	168	1.1482		1.1641	1.175	0.19		0.11	1.52	G 721
BRUXELLES	V	168	0.0033		0.0041	0.022	0.16		0.20	1.07	G 721
BRUXELLES	V	80	1.1499		1.1643	1.158	-0.18		0.06	-0.24	G 730
BRUXELLES	V	80	0.0040		0.0055	0.024	0.19		0.27	1.19	G 730
BRUXELLES	V	158	1.1500		1.1642	1.167	0.30		0.25	-0.44	G 804
BRUXELLES	V	158	0.0022		0.0032	0.017	0.11		0.15	0.84	G 804
BRUXELLES	V	50	1.1477		1.1642	1.152	-0.35		-0.14	-1.01	G 761
BRUXELLES	V	50	0.0025		0.0043	0.018	0.13		0.21	0.91	G 761
BRUXELLES	V	76	1.1489		1.1642	1.156	0.20		0.05	0.38	A 210
BRUXELLES	V	76	0.0039		0.0043	0.020	0.19		0.21	0.99	A 210
BRUXELLES	V	70	1.1503		1.1642	1.186	-0.23		-0.23	-0.20	L 258
BRUXELLES	V	70	0.0061		0.0069	0.031	0.30		0.34	1.51	L 258
BRUXELLES	V	80	1.1403		1.1643	1.160	0.71		0.21	-0.61	L 298
BRUXELLES	V	80	0.0037		0.0051	0.025	0.19		0.25	1.25	L 298
BRUXELLES	V	1694	1.1443	1.140	1.1643	1.113	-0.08	0.43	-0.50	-0.31	AA145
BRUXELLES	V	1694	0.0051	0.014	0.0075	0.038	0.25	0.72	0.37	1.99	AA145
BRUXELLES	V	916	1.1575	1.252	1.1616	1.202	-0.49	0.66	-0.42	-2.14	AA160
BRUXELLES	V	916	0.0089	0.024	0.0134	0.071	0.18	0.49	0.27	1.45	AA160
BRUXELLES	V	522	1.1456	1.190	1.1647	1.153	-1.02	-3.26	-0.27	-1.10	AA191
BRUXELLES	V	522	0.0052	0.017	0.0065	0.032	0.26	0.84	0.32	1.60	AA191
TRANS EUROPEAN PROFILE											
BIDSTON	V	200	1.1676		1.1572	1.166	0.36		0.17	-0.93	G 721
BIDSTON	V	200	0.0021		0.0030	0.016	0.10		0.15	0.77	G 721
CAMBRIDGE	V	60	1.1359		1.1366	1.257	-3.96		-0.14	0.98	G 721
CAMBRIDGE	V	60	0.0090		0.0133	0.065	0.46		0.67	2.98	G 721
HERSTM.	V	114	1.1409		1.1491	1.161	0.55		0.17	-1.91	G 721
HERSTM.	V	114	0.0023		0.0036	0.018	0.12		0.18	0.89	G 721
OOSTENDE	V	104	1.1375		1.1688	1.196	0.48		0.27	-0.33	G 730
OOSTENDE	V	104	0.0031		0.0043	0.021	0.15		0.21	0.99	G 730
WALFERD.	V	72	1.1524		1.1632	1.140	0.47		-0.05	-2.26	G 804
WALFERD.	V	72	0.0043		0.0056	0.031	0.22		0.28	1.55	G 804
WALFERD.	V	110	1.1399		1.1540	1.155	0.18		0.27	0.18	A 206
WALFERD.	V	110	0.0033		0.0044	0.021	0.17		0.22	1.04	A 206

Table 1 (Continued)

Dynamical Effects of the Earth's Liquid Core on the Tesseral Diurnal Waves

B. Gravimetric Measurements - Vertical Component

Recent Tidal Gravity Profiles / Provisional Results/

Trans European Profile (continued)

STRASBOURG	V	78	1.1342	1.1442	1.170	0.12	-0.36	-0.87	G 730
STRASBOURG	V	78	0.0021	0.0028	0.016	0.11	0.14	0.78	G 730
STRASBOURG	V	76	1.1372	1.1552	1.168	0.15	-0.04	3.52	A 206
STRASBOURG	V	76	0.0022	0.0033	0.021	0.11	0.17	1.00	A 206
CLERMONT/F	V	98	1.1569	1.1720	1.195	0.79	-0.09	-1.99	G 804
CLERMONT/F	V	98	0.0025	0.0033	0.016	0.13	0.16	0.78	G 804
GRASSE/NI	V	96	1.1439	1.1583	1.172	0.39	0.22	2.18	G 804
GRASSE CE	V	96	0.0039	0.0058	0.030	0.20	0.29	1.49	G 804
BORDEAUX	V	86	1.1567	1.1544	1.137	0.91	0.06	-1.22	G 804
BORDEAUX	V	86	0.0027	0.0045	0.021	0.14	0.22	1.05	G 804
CHUR	V	130	1.1470	1.1652	1.165	-0.09	0.30	-0.15	G 804
CHUR	V	130	0.0018	0.0028	0.013	0.09	0.14	0.64	G 804
TORINO	V	90	1.1199	1.1585	1.142	-2.21	-0.76	-0.91	G 730
TORINO	V	90	0.0036	0.0051	0.025	0.18	0.25	1.25	G 730
BONN	V	42	1.1438	1.1769	1.181	1.02	-0.70	0.68	A 210
BONN	V	42	0.0080	0.0141	0.086	0.41	0.69	4.20	A 210
HANNOVER	V	32	1.1446	1.1574	1.168	-0.46	-0.73	1.36	L 260
HANNOVER	V	32	0.0045	0.0077	0.039	0.23	0.39	1.89	L 260
FAEROE	V	78	1.1953	1.1452	1.138	1.34	1.38	-4.30	G 730
FAEROE	V	78	0.0041	0.0063	0.030	0.20	0.32	1.50	G 730

G GEODYNAMICS L LACOSTE ROMBERG
AA ASKANIA GS 11 A ASKANIA GS 15

can thus be derived with the highest precision by a harmonic analysis of the very long series of data available (tables 1A and 1B).

Moreover the theoretical amplitude of the O_1 wave is comparatively large as it is one of the main tidal waves (with M_2 and K_1), being :

in inclination	0''006;
in gravity	31 µgal; and
in geoid radial deformation	10 cm.

These amplitudes have to be multiplied by sin 2ϕ for gravity and radial deformation (ϕ is the latitude of the place considered) and by cos 2ϕ or sin ϕ for north-south or east-west inclination components.

We are therefore of the opinion that the excellent results obtained for O_1 allow us to derive the static value of Love parameters from Earth ground observations as follows:

$$\gamma(O_1) = 0.6788 \pm 0.0056,$$

$$\delta(O_1) = 1.1628 \pm 0.0008,$$

$$k = 0.317 \pm 0.011 ,$$

$$\boxed{h = 0.638 \pm 0.017} ,$$

and

$$k/h = 0.497 \pm 0.022.$$

It is to be observed that a theoretical check exists for the ratio k/h, which is:

$$k/h \leq \frac{3}{2} \frac{C}{Ma^2} = 0.499.$$

The equal sign corresponds to homothetic deformations (MELCHIOR 1973,volume 3-p.114).

For the other tesseral diurnal tidal waves, the Earth core dynamical effects have to be taken into account. The experimental results given in table 1 demonstrate with confidence their reality.

The following values of h are then derived:

For wave K_1 with period 23^h56^m $\quad h = 0.474 \pm 0.015$

For wave P_1 with period 24^h04^m $\quad h = 0.574 \pm 0.076$

(see table 2).

Table 2

Experimental Results

/28,568 days of registration/

	$\gamma = 1 + k - h$	$\delta = 1 + h - \frac{3}{2}k$	h	k	k/h
K1 165.555	0.7429±0.0045	1.1485±0.0028	0.474±0.015	0.217±0.011	0.458±0.026
P1 163.555	0.7054±0.0157	1.1550±0.0300	0.574±0.076	0.279±0.068	0.487±0.119
O1 145.555	0.6788±0.0056	1.1628±0.0008	0.638±0.017	0.317±0.011	0.497±0.022
Q1 135.655	0.6504±0.0207	1.1588±0.0095			
THEORETICAL MODELS					
**********					
MOLODENSKY MODEL 1					
K1 165.555	0.734	1.136	0.521	0.256	0.491
P1 163.555	0.699	1.154	0.594	0.294	0.494
O1 145.555	0.688	1.161	0.617	0.305	0.494
MOLODENSKY MODEL 2					
K1 165.555	0.730	1.142	0.528	0.258	0.489
P1 163.555	0.697	1.158	0.593	0.290	0.489
O1 145.555	0.686	1.164	0.614	0.300	0.488

γ: /1/ 14 STATIONS EQUIPPED WITH VM QUARTZ PENDULUMS-18056 DAYS OF REGISTRATION/

δ: /2/ 18 STATIONS EQUIPPED WITH GRAVIMETERS - 10512 DAYS OF REGISTRATION/

The fundamental parameter determining the resonance frequency in the diurnal tesseral waves is the *flattening* of the core which determines the possible movements with respect to the mantle.

As a first approximation one cannot do anything other than to adopt the hydrostatic flattening derived from Clairaut theory : 1/393 (BULLEN & HADDON 1973) which corresponds to a difference in the equatorial and polar semi-diameters of the core of 9 km, the equatorial radius best value being now determined as

$$R = 3483 \text{ km} \pm 3 \text{ km}.$$

It is to be hoped that an observed flattening will be very soon derived directly from seismology.

Very precise Earth tide measurements of very long duration could permit us to determine the resonance frequency and obtain more information concerning core motions.

Figure 1 shows that, according to a very elementary Molodensky model, this frequency is near to the ψ_1 line in the tidal spectrum.

Analysis of long records has recently been made to try to determine the amplitudes of the secondary waves ψ_1, ϕ_1, π_1, J_1, Q_1, M_1 and OO_1 in the tidal spectrum.

Unfortunately the mean square errors are still high as their theoretical amplitude is extremely small but some preliminary results are encouraging. Special careful analysis is being undertaken to improve these results.

Moreover it is to be noted that in all the European trans-continental gravity profiles, the phase of the O_1 wave is not significantly different from zero, even in the Faeroe Islands and at a near-shore coastal station like Oostende.

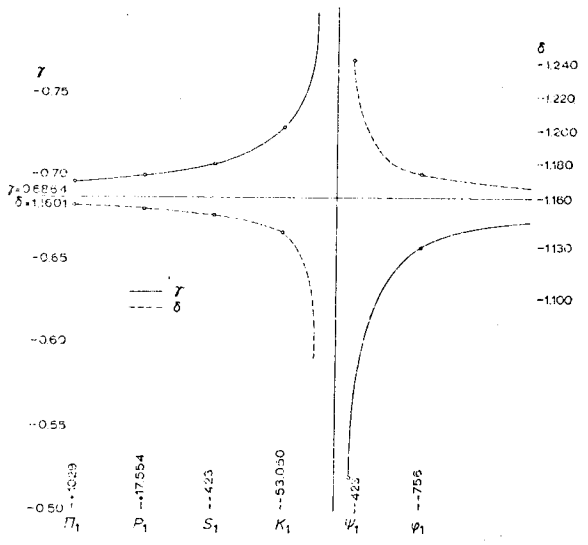

Figure 1.

2. Semi-diurnal Waves

The results of many stations are now available, e.g., see presentations at the IUGG Moscow General Assembly in 1971, and at the 7th International Symposium on Earth Tides at Sopron in 1973; also see tables 1 and 3. Only some very typical examples of the perturbations due to the loading and attraction effects of the oceanic tides will be given here: we have selected some coastal or insular stations, and compare the amplitude factors obtained for the diurnal O_1 wave with the main semi-diurnal wave M_2:

Table 3

Semi - Diurnal Tidal Waves as Given in Europe for the Vertical Component

		N	M2	N2	S2	K2	M2	N2	S2	K2	INSTR
			AMPLITUDE FACTORS				PHASE				
BRUXELLES	V	606	1.1865	1.178	1.207	1.154	3.16	2.52	-0.69	1.96	G 84
BRUXELLES	V	606	0.0013	0.006	0.003	0.008	0.06	0.31	0.13	0.41	G 84
BRUXELLES	V	168	1.1793	1.182	1.199		3.16	2.10	1.84		G 721
BRUXELLES	V	168	0.0023	0.012	0.004		0.11	0.59	0.19		G 721
BRUXELLES	V	80	1.1771	1.157	1.210		3.16	3.89	0.89		G 730
BRUXELLES	V	80	0.0030	0.014	0.006		0.14	0.67	0.28		G 730
BRUXELLES	V	158	1.1821	1.186	1.205		3.16	2.80	0.86		G 804
BRUXELLES	V	158	0.0017	0.009	0.003		0.08	0.45	0.16		G 804
BRUXELLES	V	50	1.1704	1.134	1.200		3.16	3.62	0.09		G 761
BRUXELLES	V	50	0.0029	0.012	0.008		0.14	0.60	0.40		G 761
BRUXELLES	V	76	1.1991	1.152	1.218		3.16	3.28	1.58		A 210
BRUXELLES	V	76	0.0032	0.015	0.005		0.16	0.74	0.25		A 210
BRUXELLES	V	70	1.1903	1.181	1.209		3.16	1.60	1.35		L 258
BRUXELLES	V	70	0.0046	0.022	0.007		0.22	1.06	0.36		L 258
BRUXELLES	V	80	1.1872	1.160	1.206		3.17	4.55	2.32		L 298
BRUXELLES	V	80	0.0031	0.015	0.006		0.15	0.75	0.30		L 298
BIDSTON	V	200	1.1600	1.188	1.184		0.99	0.15	1.02		G 721
BIDSTON	V	200	0.0017	0.009	0.003		0.09	0.43	0.16		G 721
CAMBRIDGE	V	60	1.2069	1.148	1.130		4.21	4.87	-0.20		G 721
CAMBRIDGE	V	60	0.0052	0.027	0.010		0.25	1.35	0.49		G 721
HERSTMONC.	V	114	1.1213	1.143	1.144		0.99	0.12	2.06		G 721
HERSTMONC.	V	114	0.0012	0.006	0.003		0.06	0.30	0.13		G 721
OOSTENDE	V	104	1.0753	1.085	1.139		4.61	0.77	4.65		G 730
OOSTENDE	V	104	0.0025	0.012	0.005		0.13	0.61	0.24		G 730
WALFERD.	V	72	1.1867	1.173	1.192		2.37	3.19	0.93		G 804
WALFERD.	V	72	0.0035	0.020	0.006		0.17	0.98	0.30		G 804
WALFERD.	V	110	1.1854	1.184	1.192		2.47	3.03	1.12		A 206
WALFERD.	V	110	0.0022	0.011	0.004		0.11	0.53	0.20		A 206

T a b l e 3 (Continued)

Semi - Diurnal Tidal Waves as Given in Europe for the Vertical Component

STRASBOURG	V	78	1.1693	1.154	1.189	1.94	2.37	1.52	G 730
STRASBOURG	V	78	0.0018	0.010	0.003	0.09	0.50	0.15	G 730
STRASBOURG	V	76	1.1842	1.207	1.185	1.96	3.50	0.36	A 206
STRASBOURG	V	76	0.0022	0.013	0.004	0.11	0.61	0.20	A 206
CLERMONT/F	V	98	1.2038	1.202	1.217	3.85	2.26	2.30	G 804
CLERMONT/F	V	98	0.0014	0.007	0.003	0.07	0.32	0.13	G 804
GRASSE/NI	V	96	1.1816	1.159	1.191	2.47	1.78	1.63	G 804
GRASSE CE	V	96	0.0017	0.008	0.003	0.08	0.43	0.16	G 804
BORDEAUX	V	86	1.2044	1.137	1.230	7.36	7.67	4.42	G 804
BORDEAUX	V	86	0.0028	0.013	0.007	0.14	0.65	0.33	G 804
CHUR	V	130	1.1894	1.167	1.195	2.23	2.71	1.48	G 804
CHUR	V	130	0.0014	0.006	0.003	0.07	0.31	0.14	G 804
TORINO	V	90	1.1790	1.175	1.192	1.68	1.69	0.92	G 730
TORINO	V	90	0.0027	0.014	0.005	0.13	0.66	0.23	G 730
BONN	V	42	1.2025	1.189	1.231	1.85	1.68	-0.91	A 210
BONN	V	42	0.0075	0.044	0.018	0.36	2.12	0.86	A 210
HANNOVER	V	32	1.1801	1.191	1.187	1.29	3.43	-0.23	L 260
HANNOVER	V	32	0.0033	0.015	0.007	0.16	0.74	0.35	L 260
HANNOVER	V	32	1.1825	1.170	1.204	1.29	2.14	0.22	L 298
HANNOVER	V	32	0.0045	0.021	0.010	0.22	1.02	0.46	L 298
FAEROE	V	78	1.5770	1.494	1.470	0.15	3.46	-6.99	G 730
FAEROE	V	78	0.0059	0.027	0.013	0.21	1.02	0.49	G 730

1)	*Gravity Tide*	$\delta(O_1)$	$\delta(M_2)$
	Spitsbergen	1.12	0.57
	Faeroe	1.14	1.57
	Oostende (B)	1.17	1.07
	Kerguelen	1.17	1.00
2)	*Clinometric Tide*	$\gamma(O_1)$	$\gamma(M_2)$
	Sclaigneaux (B)	0.68	0.8
	Spitsbergen	0.62	5.5

Such results for M_2 cannot be directly interpreted in terms of Love numbers.

Corrections due to the oceanic effects must be calculated according to procedures described by several authors (FARREL 1972; BOWER 1970; KUO 1969). Then the corrected results available show a tendency of M_2 to agree with those previously described of O_1. However such a procedure will only be successful if we have at our disposal a correct model of the cotidal charts for all the oceans.

This is far from being the case and therefore J.T. Kuo proposes to solve the inverse problem; that

is, to try to improve these cotidal charts on the basis of shore and island solid Earth tide measurements. A first application of this technique has recently been presented by JACHENS & KUO (1973). But obviously very much has to be done to make progress in that way. Precise observations of Earth tides are needed in all parts of the world and not only, as at present, in some restricted areas (North America, Europe, Japan).

Trans-World tidal gravity profiles are just now expanded to build such a network which would serve as the reference for satellite mapping of the solid Earth and oceans.

Table 4 gives the semi-amplitude of radial deformation of the geoid corresponding to the 18 main waves. It must be observed that in practice, the maximum deviation will never reach the total of the amplitudes indicated as the diurnal components have sin 2ϕ as a factor, while the semi-diurnals have $\cos^2\phi$ as factor and the long period ones have $(1 - 3 \sin^2\phi)$ as factor.

The possible deformation of the crust has been computed for the experimentally obtained value of h : 0.638.

It shows that a precision of 5% could be sufficient actually to ensure a correction of the measurements precise to 1 cm. The calibration of the tidal instruments is presently precise to 1% or sometimes 0.5%, but systematic errors of 3% or so have sometimes been found and accordingly corrected. This problem of calibration cannot be underestimated (see Annex).

3. Conclusions

The main needs at present are:

1) A correct model of the Earth's core for the evaluation of resonance effects on diurnal tidal waves.

2) A correct model of the Earth's crust and the oceanic cotidal charts for the evaluation of semi-diurnal deformations.

3) Well calibrated instruments correctly installed in a world-wide net of Earth tide stations to check the model results.

4. Annex

Some Remarks Concerning Earth Tide Instruments

The tidal amplitudes are so small that much care has to be taken in the installation and the maintenance of the instruments to avoid systematic influences and to avoid a too high level of noise.

Unfortunately many instruments have not been installed in optimum conditions and the results obtained at these stations have to be discarded in a general analysis.

The criteria to be applied to check the quality of the stations are as follows.

1. *Gravimeters*

Amplitudes to be measured are between 1 µgal and 45 µgal; they must be installed in thermostatized underground rooms (depth from 2 to 3 m).

Levels insensitivity points must have been checked, calibrations must have been made every week and must show a fairly smooth linear change with time or no change at all.

Results of table 1B obtained with 11 different instruments at Bruxelles show the possible agreement to be obtained.

2. *Clinometers*

Amplitudes to be measured are between 0''0002 and 0''0090; they must be installed at a minimum depth of 50 m and completely isolated from any thermic influence including those due to weekly maintenance.

Table 4

Radial Deformations in Centimetres

H = 0.638			
	FREQUENCY	GEOID	CRUST
DIURNAL COMPONENTS		AMPLITUDE FACTOR SIN 2ϕ	
Q1	-13.3986609	1.93	1.23
O1	-13.9430356	10.08	6.43
M1	-14.4966939	0.79	0.50
P1	-14.9589314	4.69	2.99
S1	-15.0000020	0.11	0.07
K1	-15.0410686	14.18	9.05
J1	-15.5854433	0.79	0.50
001	-16.1391017	0.71	0.45
TOTAL		33.07	21.07
SEMI DIURNAL COMPONENTS		AMPLITUDE FACTOR $\cos^2\phi$	
2N2	27.8907130	0.61	0.39
N2	28.4397295	4.65	2.96
M2	28.9841042	24.30	15.50
L2	29.5284789	0.69	0.44
S2	30.0000000	11.30	7.21
K2	30.0821373	3.08	1.96
TOTAL		44.63	28.43
LONG PERIOD COMPONENTS		AMPLITUDE FACTOR /1-3 $\sin^2\phi$ /	
SA	0.0410668	0.31	0.20
SSA	0.0821373	1.95	1.24
MM	0.5443747	2.21	1.41
MF	1.0980331	4.19	2.67
TOTAL		8.66	5.52

They must be provided with an automatic calibration system and their calibration must show a fairly smooth linear change with time or no change at all.

Results of table 5 obtained in the same laboratory with different instruments show possible agreement or discrepancy obtained.

3. *For All Types of Instruments*

Diurnal waves results (K_1 P_1 O_1) must have have been published as they reflect particularly well the environment qualities.

5. References

BOWER, D.R. 1970. Some Numerical Results in the Determination of the Indirect Effect. (Presented to 6th Symposium on Earth Tides,Strasbourg) *Obs.R.Belg.Comm.A9,S.géophys.* 96,106-112.

BULLEN, K.E. & HADDON, R.A.N. 1973. The Ellipticities of Surfaces of Equal Density Inside the Earth. *Physics of the Earth and Plan.Int.* 7,199-202.

T a b l e 5
Comparison of Three Different Instruments at Walferdange Underground Laboratory

	N	K1	P1	O1	Q1	K1	P1	O1	Q1	INSTR.
WALFERD.1 EW	1176	0.7591	0.737	0.6816	0.637	-3.09	-1.38	0.88	-3.37	VM 42
WALFERD.1 EW	1176	0.0042	0.014	0.0057	0.030	0.33	1.11	0.49	2.75	VM 42
WALFERD.2 EW	870	0.7553	0.728	0.6395	0.602	-5.13	-7.34	-4.09	5.53	VM 12
WALFERD.2 EW	870	0.0058	0.019	0.0078	0.040	0.44	1.50	0.71	3.88	VM 12
WALFERD.3 EW	320	0.7338	0.764	0.6727	0.590	-4.21	-2.91	-7.60	-17.72	TSB 16
WALFERD.3 EW	320	0.0178	0.057	0.0241	0.121	1.40	4.26	2.05	11.79	TSB 16

	N	M2	N2	S2	K2	M2	N2	S2	K2	INSTR.
WALFERD.1 EW	1176	0.8771	0.949	0.730	0.763	-8.53	-4.83	-13.90	-12.40	VM 42
WALFERD.1 EW	1176	0.0020	0.010	0.004	0.012	0.13	0.64	0.31	0.90	VM 42
WALFERD.2 EW	870	0.9205	0.956	0.774	0.793	-9.71	-6.43	-13.96	-13.15	VM 12
WALFERD.2 EW	870	0.0021	0.011	0.004	0.013	0.13	0.68	0.33	0.97	VM 12
WALFERD.3 EW	320	0.8054	0.865	0.753	0.750	-8.94	-3.62	-13.13	-10.23	TSB 16
WALFERD.3 EW	320	0.0053	0.026	0.011	0.037	0.38	1.74	0.85	2.83	TSB 16
WALFERD.1 NS	1110	0.6261	0.662	0.630	0.626	-5.10	-5.16	-1.91	-1.57	VM 10
WALFERD.1 NS	1110	0.0028	0.015	0.006	0.017	0.25	1.28	0.51	1.50	VM 10
WALFERD.2 NS	1240	0.6556	0.695	0.635	0.643	0.18	-2.82	7.92	2.11	VM 56
WALFERD.2 NS	1240	0.0024	0.013	0.005	0.014	0.21	1.06	0.45	1.29	VM 56
WALFERD.3 NS	310	0.6041	0.645	0.747	0.677	-6.95	-14.26	4.22	-28.92	TSB 15
WALFERD.3 NS	310	0.0080	0.041	0.017	0.056	0.75	3.64	1.33	4.75	TSB 15

VM VERBAANDERT-MELCHIOR QUARTZ PENDULUM
TSB TSUBOKAWA ELECTROMAGNETIC PENDULUM
N NUMBER OF DAYS

FARREL, W.E. 1972. Deformation of the Earth by Surface Loads. *Revs.geophys. and space phys.* 10, 761-797.

JACHENS, R.C. & KUO, J.T. 1973. The O_1 Tide in the North Atlantic Ocean as Derived from Land-Based Tidal Gravity Measurements. *7th Symposium on Earth Tides.* Sopron.

KUO, J.T. 1969. Static Response of a Multilayered Medium Under Inclined Surface Loads. *J.geophys. Res.* 74,3195-3206.

MELCHIOR, P. 1973. *Physique et Dynamique planetaires, Vol. 3 et 4.* Vander, rue Defacqz 21, 1050 Bruxelles.

6. Discussion

SAKUMA: Presently it is believed that the velocity of gravitational waves is equal to the velocity of light, but this has not yet been proved. Do you think it might be possible to determine this value by measuring the phase of the Earth tides due to the sun? Because gravitational waves should take about eight minutes to the Earth from the sun.

MELCHIOR: This is a difficult question because of the precision of phase. We can barely investigate the diurnal wave in that case. The speed of the paper is one limiting factor. It is 2-3 cm per hour (or 3 mm per 6 minutes). It could be done. Tidal measurements do not use high speed recorders as we are mainly concerned with long period waves.

KAULA: Your paper does not mention the use of pressure sensors at the bottom of the oceans. What are the possibilities in this area?

MELCHIOR: I have no personal experience of these measurements, but I do know measurements are being made for the improvement of tidal charts at amphidromic points. But I have no personal comments.

LAMBECK, K.
Institut de Physique du Globe
Université Paris VI
quai Saint-Bernard 75230 Paris
&
Groupe de Recherches de Géodésie Spatiale
Centre National d'Etudes Spatiales
91 Bretigny sur Orge
France

Proc. Symposium on Earth's Gravitational Field & Secular Variations in Position (1973), 522-528.

DETERMINATION OF EARTH AND OCEAN TIDES FROM THE ANALYSIS OF SATELLITE ORBITS

1. Solid Earth Tides

The elastic deformation of the Earth due to the variable lunar and solar attraction has been reviewed most recently by SLICHTER (1972). Observations of these deformations provide estimates of the Earth's mean elastic parameters. If the potential of the attracting force U_n is harmonic in degree n, the elastic response is also assumed to be harmonic in degree n, and in the classical definition of LOVE (1909), (see also JEFFREYS 1962) the additional potential resulting from the deformation is defined at the Earth's surface R, as

$$\Delta U_n = k_n U_n(R)$$

or, at a point r exterior to the Earth, as

$$\Delta U_n(r) = k_n \left(\frac{R}{r}\right)^{n+1} U_n(R) = k_n \left(\frac{R}{r}\right)^{2n+1} U_n(r)$$

The principal tidal terms occur for degree 2. The harmonics of zero order give the zonal tides, the first order harmonics the diurnal tides and the second order harmonics the semi-diurnal tides. Similar definitions define the actual deformation at the Earth's surface. Thus the radial deformation at the surface is defined as $h_n U_n(R)/g$ (g is gravity at the surface) and the horizontal deformations are in longitude (λ) $\frac{\ell_n}{g} \frac{\partial U_n}{\partial \phi}(R)$, and in latitude ($\phi$) $\frac{\ell_n}{g \cos \phi} \frac{\partial U_n}{\partial \lambda}(R)$. The Love numbers h_n k_n ℓ_n are integral measures of the Earth's elastic properties and relate in a complex manner to such parameters as the density, bulk modulus and rigidity variations throughout the Earth. They present most satisfactory transfer parameters between complex theory on the one hand and refined measurements on the other hand, although their interpretation is not always free from ambiguity.

In their classical definition, the Love numbers define the response of a radially symmetric, perfectly elastic, Earth to the perturbing potentials. This theoretical response is now best determined from seismology where the elastic parameters can be measured directly as a function of depth. These calculations have been most recently performed by FARRELL (1972). This study, as well as earlier ones, showed that the Love numbers are not very sensitive to the choice of mantle model; an oceanic type upper mantle giving almost identical results as a continental type upper mantle. Thus, if the theoretical response corresponded to reality, there would be little value in observing the solid tides as they provide only an insensitive global measure of the elasticity of the Earth. Before the development of seismology, however, solid tide observations played an important role in establishing the existence of the dense and liquid core.

The theoretical response is strongly modified or influenced by the fluid parts of the Earth, and to a lesser extent by the Earth's anelastic properties. A modification of some interest is the possible resonance effect due to inertial coupling between the elastic mantle and fluid core as propounded by the theories of JEFFREYS & VICENTE (1957) and which predict, for some of the diurnal tides, a rapid change in the value of k_2 with frequency. Solid tide observations have until now, not been very successful in distinguishing between the variously proposed models mainly because the oceans perturb the tide observations (SLICHTER 1972; BLUM et al 1973). In any case, it would appear that these resonances may tell us more on how to solve an interesting mathematical problem rather than tell us about the physics of the coupling mechanism itself.

The Earth is not a purely elastic body, for if it were, it would still be vibrating under the combined effect of all the earthquakes since its origin. Energy is therefore dissipated, and in the case of the tidal problem this dissipation results in a slight delay in the response to the attracting potential. Observation of this lag is of greater intrinsic value than the Love numbers themselves as it provides a measure of the Earth's global imperfections in elasticity at the tidal frequencies and provides a key parameter in the understanding of the evolution of the Earth-Moon system. Observations of this lag have until now not been particularly conclusive also because the measurements are perturbed by the ocean tides.

2. Ocean Tides

Ocean tides have been reviewed recently by HENDERSHOTT & MUNK (1970) and HENDERSHOTT (1973). Long records of ocean tides exist along many of the world's coast lines and these are extremely valuable for predicting the tides locally. But such observations are very much influenced by the coastline configurations and the shallow coastal seas and they are hardly representative of the mid-ocean tides. The best observational data of the latter comes from island stations that are little disturbed by local sea floor topography and all such records show that the undisturbed tide is little more than a meter. The available island measurements do not suffice for establishing the global pattern accurately, and the recent development of pressure tide gauges for measuring the tides in the open sea have made no impact yet on the global tide solutions. Our present knowledge of the open ocean tides comes from the more or less complete solutions of the Laplace tidal equations and a number of solutions for the M_2 tide (the principal semi-diurnal lunar tide) have been published recently. PEKERIS & ACCAD (1969) give solutions assuming a rigid Earth with, as boundary conditions, an impermeable coastline and allowing explicitly for dissipation in shallow seas. HENDERSHOTT (1972) allows for the effect of the tidal yielding of the solid Earth on the ocean tide and also attempts to evaluate the effect of the Earth's deformation under the variable ocean load (see also FARRELL 1972). Hendershott's boundary conditions are that the tide must correspond to the observed coastal values and dissipation is allowed for by allowing flow normal to the coastlines. The solutions of PEKERIS & ACCAD and of HENDERSHOTT agree in many areas but important discrepancies exist in, for example, the Pacific Ocean, pointing to the need for both improved theory and for more observational data. The S_2 ocean tide (the principal semi-diurnal solar tide) has been computed by BOGDANOV & MAGARIK (1967). No numerical solutions appear to exist for the other semi-diurnal tides or for the diurnal tides, although DIETRICH (1944) gives empirical cotidal charts for the O_1 (a nearly diurnal tide of solar origin) and K_1 (also nearly diurnal and of solar and lunar origin) tides as well as observed aplitudes along the coastlines and for some island sites.

3. Solid - Ocean Tide Interaction

The importance of the ocean tide interference with the solid tide has been demonstrated by the variable results obtained from surface measurements (for example, KUO et al 1970; PERTSEV 1969; BLUM & HATZFELD 1970; BERGER & LOVBERG 1970; SLICHTER 1972). The ocean loading of the continents appears to perturb all tide measurements, even those in the middle of the continents and although local tides are oftem most important (for example, LAMBERT 1970) even very distant tides will contribute to the observed combined tide (KUO et al 1970; PERTSEV 1969). In general, the ocean tides are not well enough known to be able to correct for this loading and improvements in the solid tide studies can only come about if there is also an improvement in our knowledge of the ocean tide (HENDERSHOTT & MUNK 1970). We cannot separate fully, at present, the fluid and solid tides through lack of mathematical completeness of the ocean tide solutions and through lack of global observational ocean tide data in particular for the components other than the principal components. Progress in interpreting the solid tidal measurements in terms of phase lags, resonances or geological variations, can only be achieved by a concomitant progress in ocean tide solutions. It is possible to use the Earth tide measurements as constraints in these solutions in the sense that any departures from a theoretical response can be used as an integral of the ocean tide. The value of such constraints still has to be proved but in view of the numerical solutions extreme sensitivity to small changes in boundary conditions, it would seem probable that any additional constraints will be of value. The foregoing remarks are equally valid for tidal studies from terrestrial measurements as for tidal studies from satellite orbit analyses, the only difference being that the two provide different constraints and as such the two methods are entirely complementary (LAMBECK et al 1973; 1974).

4. Satellite Methods for Tidal Studies

The tidal potential $\Delta U(r)$ at the satellite causes an additional force function that has to be taken into account when the satellite's equations of motion are integrated. This potential introduces perturbations in the motion of close Earth satellites and KAULA (1964; 1969) has given the necessary formalism. The frequencies of these tidal perturbations are governed by the frequencies of the satellite motion around the Earth and the perturbing body's motion in space and the principal perturbations will tend to group around the principal terms in the lunar and solar motion. Thus the semi-diurnal M_2 tide will give perturbations with periods near fourteen days and the solar S_2 tide will give perturbations with periods near six months. Also, as the satellite measures the integral effect of the tidal potential, the longer the period of the perturbation, the larger will be its amplitude. Thus the S_2 tide even though on the Earth's surface it has less than one half the amplitude of the M_2 tide it will cause perturbations in the satellite motion an order of magnitude larger than the M_2 perturbations. In the special cases where the satellite parameters and the Sun's or Moon's elements combine so as to give very long period orbital perturbations, tides that are very small on the Earth can give rise to very large orbital perturbations. The amplitudes of the tidal perturbations are proportional to the Love numbers. For most discussions of the tides, only the potential component of degree 2 is considered as the others are small. In particular, at the satellite height the potential decreases rapidly with increasing degree due to the term $(R/r)^{2\ell+1}$ in $\Delta U(r)$. Thus with the satellite methods it is k_2 that is observed. The difference between the observed phase of the perturbation and the phase of the perturbing potential assuming a perfectly elastic Earth, gives a measure of the phase lag. This lag has a value of at most one or two degrees

and is very much more difficult to observe with confidence than k_2. Some typical periods and amplitudes of the tidal orbital perturbations are given in Table 1.

Due to the ocean-continent distribution and the variable sea floor topography, the ocean tides, when expressed in terms of spherical harmonics will contain all harmonics of degree zero to infinity but the convergence appears to be rapid (see the solution of HENDERSHOTT 1972). This tide generates a potential which is readily expressed by a surface density layer representation and which gives an additional term to the force function acting on the satellite. We would expect that this ocean tide would generate perturbations of the same frequency as the solid tide due to that term in the ocean tide expansion that has the same degree and order as the solid tide. In addition, we could expect further perturbations resulting from the other harmonics in the ocean tide expansion. But most of these further perturbations are of short period - near the period of revolution of the satellite about the Earth - and as such do not build up into measurable perturbations (LAMBECK et al 1973). If the tidal potential is of degree 2 and order m, then the principal ocean tide perturbations, having the same frequencies as the solid tide perturbations, are caused by the ocean harmonics of degree and order 2,m ; 4,m ; 6,m etc, with a rapid decrease in importance. Table 2 gives some orders of magnitude. In general, the ocean perturbations are equal to about 10% of the solid tide. One observes therefore, a combined solid-ocean tide. Or, if the perturbation in an element ε due to the principal lunar tide is written as

$$(\delta\varepsilon)_{st} = k_2 \phi \cos \gamma$$

the ocean tide perturbation with the same frequency γ is

$$(\delta\varepsilon)_{ot} = (C_{22} \psi_{22} + C_{42} \psi_{42} + C_{62} \psi_{62}) \cos \gamma$$

where the C are coefficients in the ocean tide expansion (LAMBECK & CAZENAVE 1973; LAMBECK et al 1974). We observe

$$(\delta\varepsilon)_{obs} = (k_2\phi + C_{22} \psi_{22} + C_{42} \psi_{42} + \dots) \cos \gamma$$

The factors ϕ and ψ depend on the orbital parameters and one could imagine that a separation of the k_2 and C is possible if different satellite orbits or different orbital elements are analysed. This is only partially true. The principal ocean term has exactly the same dependence on the orbital elements as the solid tide and a separation of k_2 and C_{22} is not possible. A separation of these terms from C_{42} (and eventually from C_{62} if very precise tracking data becomes available) is possible and we can imagine an iterative procedure where we solve for

$$(k_2 + \frac{\psi}{\phi}22\ C_{22}),\ C_{42} \text{ and } C_{62}$$

and introduce the last two parameters as constraints in the solution of the Laplace tidal equations and compute the value C_{22} and hence k_2. In exactly the same way, a separation of the phase lags resulting from the solid Earth and the oceans is not possible from the analysis of tidal perturbations alone and we can again envisage the above iterative approach.

5. Results

Love numbers have been estimated from orbital perturbations by KOZAI (1968), NEWTON (1968), ANDERLE (1971), DOUGLAS et al (1972), SMITH et al (1973) and LAMBECK et al (1974). Of these studies only the last considered the ocean tides. LAMBECK & CAZENAVE (1973) showed that the apparently aberrant results for Love numbers obtained by the various investigators resulted from their neglect of the ocean tide, and LAMBECK et al (1974) have applied the ocean corrections to the results of the earlier investigators to give a value for $k_2 = 0.306$ and a phase lag of 0.5 degrees (see Table 3). The latter leads to a mantle Q of about 60, a value in reasonable agreement with seismic results (LAGUS & ANDERSON 1968). The studies of LAMBECK & CAZANAVE (1973) and LAMBECK et al (1973; 1974) lead to the following conclusions:

i) There is an important interaction between Earth and ocean tides as observed from orbit analyses. Neglect of the latter tides can introduce errors in k_2 of as much as 15% and of several degrees in phase;

ii) the ocean tide models, even the comparatively well known M_2 tide, are inadequate for making the precise ocean corrections, particularly for the important diurnal tides;

iii) the solid Earth tidal parameters computed from the satellite orbits are not yet very conclusive, even when corrected for the ocean tides. This is in part due to ii) but also due to residual non-tidal perturbations remaining in the satellite orbit parameters and due to inadequate tracking data. Better results can be expected in the future if precise laser tracking data, well distributed in space and time, can be collected from the already existing satellites and from the new small and dense satellite to be launched by the Centre National d'Etudes Spatiales in 1974 for gravimetric and tidal studies;

iv) a complete separation of fluid and solid tides is not possible from the analysis of satellite orbits alone, but the ocean tidal parameters that can be estimated can be used as constraints in the numerical tide solutions. This is also the case for the surface measurements of the bodily tide but in the former case the constraints, being the harmonics of degree 2 and 4 (and possibly 6 in the future) are of a global nature whereas the surface measurements provide constraints on the regional tides;

v) the ocean tide effect on the satellite orbit is frequency dependent (due to near resonances between the forcing function and the free periods of the oceans) and as such one must analyse the satellite orbits for specific tidal terms rather than solve for a single parameter that will present some average effect as has been done by SMITH et al (1973) and DOUGLAS et al (1972) as this leads to results that have no clear physical interpretation even though they may describe well the orbital perturbations of a particular satellite. This frequency dependence also makes the approach through latitude dependent Love numbers (KAULA 1969) impractical.

6. References

ANDERLE, R. 1971. Refined geodetic results based on doppler satellite observations. *US Naval Weapons Laboratory, Technical Report. TR - 2889.*

BERGER, J. & LOVBERG, R. 1970. Earth strain measurements with a laser interferometer. *Science* 170,286.

Table 1
Amplitudes and Periods of Perturbations in the inclination of GEOS-1 and GEOS-2 due to some tidal Components

Satellite	Tide	Period (days)	Δi (arcsec)
GEOS-1	M_2	11.7	0.17
GEOS-1	S_2	55.7	0.40
GEOS-1	K_1	160.7	0.95
GEOS-2	M_2	15.3	0.30
GEOS-2	S_2	432.7	4.03
GEOS-2	K_1	255.1	1.04

Table 2

Amplitudes of the Orbital Perturbations in i and Ω due to the Second and Fourth Harmonics in the Ocean M_2 Tide and Compared with the Corresponding Earth Tide

		Inclination i			Ascending Node Ω			
		Earth Tide M_2	Ocean Tide M_2		Earth Tide M_2	Ocean Tide M_2		Period (days)
			Second Harmonic	Fourth Harmonic		Second Harmonic	Fourth Harmonic	
7010901	(PEOLE)	0''06	0''011	0''016	0''26	0''043	0''056	9
6503201	(BE-C)	0''16	0''025	0''017	0''19	0''032	0''002	10
6508901	(GEOS-1)	0''19	0''029	0''005	0''13	0''020	0''015	12
6406401	(BE-B)	0''31	0''051	0''009	0''12	0''019	0''018	13
6402601	(TRANSIT)	0''33	0''056	0''013	0''08	0''014	0''004	14
6800201	(GEOS-2)	0''32	0''052	0''005	0''15	0''025	0''023	15

Table 3
Summary of Results Obtined by Other Authors and Corrected for Ocean Tidal Parameters

Author	Satellite	Tidal	Element Analysed	k_2 Observed	k_2 Corrected	δ_2 Observed	δ_2 Corrected
Kozai	5900101	$K_1^m + K_1^S$	i	0.22	0.24	-5°5	-1°5
Kozai	6000902	$K_1^m + K_1^S$	i	0.31	0.34	1°3	3°7
Kozai	6206001	$K_1^m + K_1^S$	i	0.32	0.34	0°7	6°7
Newton	Mean of four Polar Satellites	M_2	i	0.27	0.30	1°5	-5°5
Newton		M_2	Ω	0.29	0.32	1°7	-5°6
Newton		S_2	i	0.34	0.36	1°6	-3°4
Newton		S_2	Ω	0.33	0.36	1°2	-3°8
Douglas et al.	6508901	$K_1 + S_2$	i	0.22	0.25		
	6800201	$K_1+S_2+P_1$	i	0.31	0.33		
Smith et al.	6502801	$K_1+S_2+P_1$	i	0.25	0.28	3°2	5°
Lambeck et al.	6800201	M_2	i + Ω	0.29			9°
		Arithmetic Mean			0.309		0°5

BLUM, P.A. & HATZFELD, D. 1970. Etude régionale de l'influence océanique sur l'inclinaison; Premiers résultats à la station de Moulis. *Comm. A-9, Ser.Geophys. 96. Obs.Roy.Belgique.* 102-105.

BLUM, P.A., HATZFELD, D. & WITTLINGER, G. 1973. Résultats expérimentaux sur la fréquence de résonance due à l'effet dynamique du noyau liquide. *C.R.Acad.Sc.Paris. Ser.B,* 277,241-244.

BOGDANOV, K.T. & MAGARIK, V.A. 1967. Numerical solutions for the world's semi-diurnal (M_2 and S_2) tides. *Dokl. Akad. Nauk SSSR, 172.* 1315-1317.

DEITRICH, G. 1944. Die schwingungssysteme der halb - und eintagigen tiden in den ozeanen. *Veroffentl. Meereskunde, Univ. Berlin.* A 41. 7-68.

DOUGLAS, B.C., KLOSKO, S.M., MARSH, J.G. & WILLIAMSON, R.G. 1972. Tidal perturbations on the orbits of Geos 1 and Geos 2. *NASA/GSFC Report X.* 553 - 72 - 475. Greenbelt, Md.

FARRELL, W.E. 1972. Deformation of the Earth by surface loads. *Rev.Geophys.Space Phys.* 10. 761-797.

HENDERSHOTT, M.C. 1972. The effects of solid Earth deformations on global ocean tides *Geophys. J. Roy.Ast.Soc.* 29. 389-402

HENDERSHOTT, M.C. 1973. Ocean tides. *Transactions American Geophysical Union.* 54. 76-86.

HENDERSHOTT, M. & MUNK, W. 1970. Tides. *Ann.Rev.Fluid Mech.* 21, 205-224.

JEFFREYS, H. 1962. *The Earth.* (4th ed.) Cambridge University Press.

JEFFREYS, H. & VICENTE, R.O. 1957. The theory of nutation and the variation of latitude. *Mon.Not.R.astr.Soc.* 117, 142-161.

KAULA, W.M. 1964. Tidal dissipation by solid friction and the resulting orbital evolution. *Reviews of Geophysics.* 2, 661-685.

KAULA, W.M. 1969. Tidal friction with latitude dependent amplitude. *Astron.Journ.* 74, 1108-1114.

KOZAI, Y. 1968. Love's number of the Earth derived from satellites observations. *Publ.Astron. Soc.Japan.* 20, 24-26.

KUO, J.T., JACHENS, R.C., EWING, H. & WHITE, G. 1970. Transcontinental tidal gravity profile across the United States. *Science.* 168, 968.

LAGUS, P.L. & ANDERSON, D.L. 1968. Tidal dissipation in the Earth and planets. *Phys.Earth Planet Interiors.* 1, 505-510.

LAMBECK, K. & CAZENAVE, A. 1973. Fluid tidal effects on satellite orbit and other temporal variations in the geopotential. *Bull.Groupe Recherches Géodesie Spatiale.* 7.

LAMBECK, K., CAZENAVE, A. & BALMINO, G. 1973. Solid Earth and fluid tides from satellite orbit analyses, in Veis, G.(ed). *The use of artificial satellites for geodesy and geodynamics.* Technical University of Athens. In press.

LAMBECK, K., CAZENAVE, A. & BALMINO, G. 1974. Solid Earth and ocean tides estimated from satellite orbit analyses *Revs.geophys.Space Phys.* 12 (May)

LAMBERT, A. 1970. The response of the earth to loading by the ocean tides around Nova Scotia. *Geophys.J.Roy.astr.Soc.* 19, 449-477.

LOVE, A.E.H. 1909. *Some problems in geodynamics.* Cambridge University Press.

NEWTON, R.R. .1968. A satellite determination of tidal parameters and Earth deceleration. *Geophys.J.Roy.astr.Soc.* 14, 505-539.

PEKERIS, C.L. & ACCAD, Y. 1969. Solution of Laplace's equations for M_2 tide in the world oceans. *Philos.Trans.Roy.Soc.*, London, Ser.A. 265. 413-436.

PERTSEV, B.P. 1969. The effect of ocean tides upon Earth tide observations. *Comm., A.9, Ser.Geophys.* 96, Obs.Roy.Belgique, 113-115.

SLICHTER, L.B. 1972. Earth Tides. In ROBERTSON, E.C.(ed.) *The Nature of the Solid Earth.* McGraw Hill, 285-320.

SMITH, D.E., DUNN, P.J. & KOLENKIEWICZ, R. 1973. Earth tidal amplitude and phase. *Nature.* 244. 498.

MUELLER, I.I.
Department of Geodetic Science
The Ohio State University
Columbus Ohio 43210
United States of America

Proc. Symposium on Earth's Gravitational Field & Secular Variations in Position (1973), 529-553.

EARTH PARAMETERS FROM GLOBAL SATELLITE TRIANGULATION AND TRILATERATION

Abstract

Results obtained from 159-station global satellite triangulation and trilateration (including Baker-Nunn, BC-4, PC-1000 camera observations, SECOR, C-Band radar and EDM distance measurements) indicate differences in the semidiameter and orientation of the Earth compared to results obtained from dynamic satellite solutions. Geoidal undulations obtained can be made consistent with dynamically determined ones at the expense of slight changes in the currently accepted parameters defining the gravity field of the level ellipsoid.

1. Introduction

The global triangulation and trilateration forming the basis of this paper was performed as part of the US National Geodetic Satellite Program. A summary of the networks involved in the adjustments reported here (solutions WN) is presented in table 1. The data for the MPS and BC networks was obtained through the National Space Science Center. The Defence Mapping Agency provided observations for the SECOR and the SA networks (Topographic Center and Aerospace Center respectively). The sources for the constraint information are listed in table 2. Figure 1 shows the combined network

Table 1

Basic Information on the OSU Solutions (Networks)

OSU Solution (Network)	No. of Stations	No. of Observations	No. of Constraints Used[8]					$^{6}\sigma_o$	[7]Reference
			Origin	Relative Position	Scale (Length)	Height	Directional		
[1]MPS	66	28,744	Inner	9	7	63	-	1.07	188
[2]BC	49	30,302	Inner	2	7	48	-	2.80	193
[3]SECOR	50	28,844	Inner	14	-	37	9	1.37	195
[4]SA	14	2,524	Inner	3	1	14	-	2.50	196
[5]WN	159	90,444	Inner	43	11	158	-	1.02	199

[1]MPS includes 14 PC-1000 stations, 15 MOTS-40 stations, 1 PTH-100 station, 7 C-Band stations, 6 European stations (8000 series), and 23 SAO stations (9000 series).

[2]BC includes all 49 stations of BC-4 Worldwide Geometric Satellite Network.

[3]SECOR includes 37 SECOR stations of the Equatorial Network and 13 collocated BC-4 Camera Stations.

[4]SA includes 9 PC-1000 stations of South American Densification Net and 5 BC-4 stations.

[5]WN includes all networks at [1], [2], [3], & [4], namely, MPS (less 1 C-Band Station 4742), BC, SECOR & SA.

[6]A posteriori standard deviation of unit weight.

[7]OSU Department of Geodetic Science Report No.

[8]No constraints imposed on station position.

Table 2

Summary of Constraint Types with the Source Information

Code	Constraint Type	Source (Agency)*
	Relative Position	
1	BC-4 - Baker-Nunn	SAO, NGS
2	BC-4 - SECOR	DMA/TC
3	BC-4 - BC-4	NGS
4	Others	OSU
	Height	
5	MSL (mean sea level heights)	CSC, NGS, NWL
6	Geoidal Undulations	OSU (RAPP 1973)
	Length (Chord)	
7	North America	NGS
8	Europe	NGS, DGFI
9	Africa	NGS
10	Australia	NGS, DNP
11	C-Band	NASA/Wallops Isl.

* CSC - Computer Sciences Corporation
NGS - National Geodetic Survey
DGFI - Deutsche Geodätisches Forschungsinstitut
NWL - Naval Weapons Laboratory
DMA/TC - Defence Mapping Agency Topographic Center
SAO - Smithsonian Astrophysical Observatory
DNP - Division of National Mapping, Australia

(WN). Different symbols indicate the various instruments utilized in the observations. Concentric symbols show collocated stations or nearby stations with relative positions from known geodetic surveys. The straight lines between some of the stations illustrate the location of the baselines.

2. Reference Ellipsoid, Origin and Orientation

The least squares adjustment of the observations was performed in terms of Cartesian co-ordinates of the tracking stations. The results are also converted into geodetic co-ordinates (latitude, longitude and height) referenced to a rotational ellipsoid of the following parameters:

$$a = 6\ 378\ 155.00 \text{ m} \quad ; \quad b = 6\ 356\ 769.70 \text{ m}.$$

The corresponding flattening is

$$f = 1/298.249\ 498\ 5 = 0.003\ 352\ 897\ 507.$$

The origin of the co-ordinate system (or the centre of the above *reference ellipsoid*) is free as determined through "inner" constraints explained in (BLAHA 1971). The orientation of the system is inherent in the optical observations, through the star positions in the SAO catalogue (referenced to the FK4 system) updated to their apparent positions at the epoch of observation, and through UT1, x and y (co-ordinates of the true pole with respect to the CIO) as derived by BIH. Thus the positive

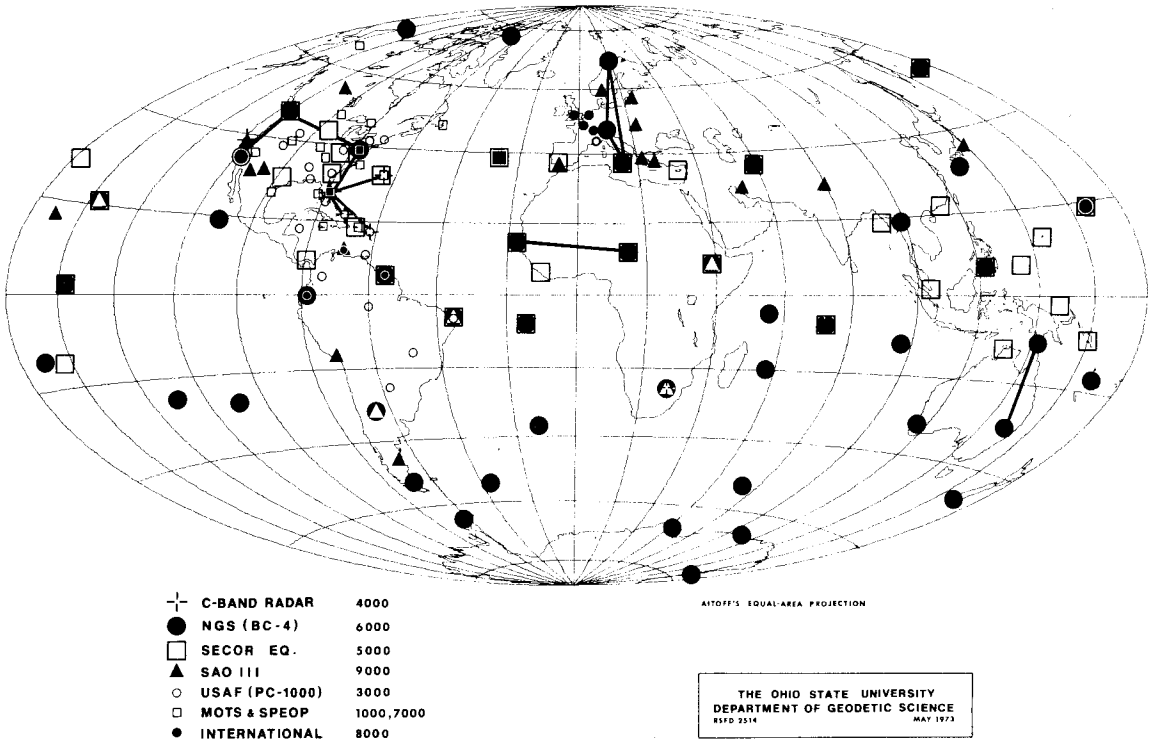

Figure 1. OSU Geometric Satellite Network (WN)

end of the axis u is in the direction of the Greenwich Mean Astronomical Meridian (and the zero geodetic meridian of the reference ellipsoid); the positive w axis passes through the Conventional International Origin (and coincides with the minor axis of the reference ellipsoid). The axis v completes the right handed co-ordinate system in the direction of the 90°(E) meridian, and with the u axis defines the plane of the average terrestrial (geodetic) equator.

3. Scale

The scale in the solution is defined through the dominating nearly 30,000 SECOR range observations, through the lengths of eight EDM (Geodimeter or Tellurometer) and three C-Band baselines, and also through a special procedure using constrained ellipsoidal heights.

3.1 SECOR Observations

The SECOR observations have an a posteriori standard deviation of ±4.1 m or approximately one part per million (MUELLER ET AL 1973b). The scale is propagated into the network through fifteen optical stations whose relative positions with respect to the nearby SECOR stations are maintained in the adjustment with their survey co-ordinate differences entered as weighted constraints.

3.2 Baselines

The available EDM and C-Band baselines are listed in table 3. The chord distances shown are entered in the adjustment as weighted constraints with weights computed from their estimated a priori

Table 3

Chord Constraints

Station-Station	Chord Distance (m)	$\sigma \times 10^6$ [1]	Source Code [2]
6002 - 6003	3 485 363.232	1.00	7
6003 - 6111	1 425 876.452	1.11	7
6006 - 6065	2 457 765.810	1.43	8
6016 - 6065	1 194 793.601	1.18	8
6063 - 6064	3 485 550.755	1.18	9
6023 - 6060	2 300 209.803	2.00	10
6032 - 6060*	3 163 623.866	2.00	10
6006 - 6016	3 545 871.454	1.00	8
3861 - 7043	1 531 562.9	1.33	7
4082 - 4050*	10 909 592	1.33	11
4082 - 4742*	7 362 142	2.00	11
4082 - 4740	1 593 106	2.00	11
4082 - 4081	1 230 691	2.00	11
4082 - 4061	2 288 026	2.00	11
4742 - 4280*	3 977 684	2.00	11

1 Used in computing the weights

2 Refer to table 2

* Rejected from the solution

standard deviations as listed in the table. The reasons for rejecting the east-west Australian tellurometer line (6032 - 6060) are explained below. Three C-Band lines were also rejected because of suspected errors in the survey co-ordinates of the terminal stations [Kauai (4742) in Hawaii and Pretoria (4040) in South Africa] needed to tie them to the nearest optical stations (9012 and 9002 respectively). Though these four lines were not constrained, at the end of the analysis, two of them (6032 - 6060 and 4082 - 4050) compared well with the lengths computed from the adjusted co-ordinates (see table 8). Thus the only station with survey co-ordinates in definite error is Kauai.

To get a feel for the quality of the EDM baselines listed in table 3, four preliminary adjustments of the BC network were performed in which the four longest scalars were individually constrained to their measured lengths, and their effect on the other (unconstrained) baselines investigated. The results are shown in table 4 in the form of the differences "adjusted - measured" lengths(Δd). Only independent lines longer than 2000 km are shown since the adjusted length of a short line, due to the geometry resulting from the high altitude of PAGEOS, the satellite used in the BC net, is not reliable. From the table it is clear that holding the east-west Australian line (3032 - 6060) to its measured value results in unreasonably larger differences of generally opposite signs than in any other case.

To verify the suspicion that something is wrong with the given measured value of line 6032 - 6060, a free adjustment was performed, in which both the origin and the scale constraints were "free" (BLAHA 1971). It is expected that the variances obtained from such an adjustment would primarily reflect the geometry of the situation. In other words, the variances of the various lengths would be due to the geometry of the network and free of the quality of the measured lengths. If the estimated variances of the measured lengths $(\sigma_d^{msrd})^2$ are added to those obtained from the free adjustment $(\sigma_d^{free})^2$, an estimate is obtained for the maximum expected variances of the length differences

Table 4

Adjusted - Given Lengths (m)

Solution	BC-8	BC-9	BC-10	BC-11
Line Fixed	6002 - 6003	6063 - 6064	6032 - 6060	6006 - 6016
6002 - 6003	0.0	-8.6	33.8	12.4
6006 - 6016	-13.3	-20.9	22.1	0.0
6063 - 6064	6.1	0.0	40.5	19.1
6023 - 6060	-9.5	-14.6	12.4	-0.7
6032 - 6060	-29.5	-36.6	0.0	-17.5
$\sum \Delta d$ (m)	-46.2	-83.6	108.8	13.3
$\sum \frac{\Delta d}{\text{length}} \times 10^6$	-2.89	-5.23	6.81	0.83

$(\sigma_d^{est})^2$. If an actual length difference is found to be 2 - 3 times greater than this estimated standard deviation, the measured length becomes suspect. The result of such analysis is shown in table 5.

From this table it is seen again that line 6032 - 6060 is out of bounds.

Another way of evaluating the effect of a scalar is through the semi-diameter of an ellipsoid best fitting the geoid resulting from a solution (see more of this in section 3.3). In this method, the undulations for each station are computed (ellipsoidal height - mean sea level height) and, after suitable transformations for shift of origin, are compared with some standard set of undulations, in this case with those in (PAPP 1973). The average difference N of these two sets of undulations is equivalent, with opposite sign, to the difference between the semi-diameter of the reference ellipsoid (a = 6 378 155 m) and that of the level ellipsoid of the same flattening to which the "standard" undulations refer.

Three sets of such comparisons were performed. One with the baselines constrained with weights corresponding to the standard deviations listed in table 3, one with all lines constrained to 1:3 M, and one with 1:30 M. Within each set, the adjustment was performed with all 6000 series EDM lines constrained and also without the line 6032-6060 (seven lines). The results are shown in table 6. In addition to the semi-diameter of the best-fitting level ellipsoid, the table also contains the

Table 5

Adjusted - Measured Lengths (Δd) from a Free Adjustment

Line	σ_d^{free} (m)	σ_d^{msrd} (m)*	$\sigma_{\Delta d}^{est}$ (m)	Δd (m)
6002 - 6003	4.2	3.5	5.5	-5.0
6006 - 6016	4.5	3.5	5.7	-17.2
6063 - 6064	4.4	4.1	6.0	2.4
6023 - 6060	4.4	4.6	6.4	-12.1
6032 - 6060	4.3	6.3	7.6	-33.1

* From table 3.

average standard deviations of a single co-ordinate ($\sigma^2 = \sigma_u^2 + \sigma_v^2 + \sigma_w^2$) as well as those of the heights (σ_H) and the ratios (adjusted - measured lengths)/lengths : $\sum(\Delta d/\text{length})$.

Table 6

Comparison of Seven- or Eight-Baseline Solutions

Solution	No. of Lines Constrained	Type of Constraint	$\sum \frac{\Delta d}{\text{length}} \times 10^6$	a (level ellipsoid) 6 378 000 + (m)	σ (m)	σ_H (m)
BC D12	8	As In	0.81	124.1 ± 11.0	6.3	8.1
BC D 2	7	table 3	0.19	118.4 ± 11.2	6.2	8.3
BC D 7	8	1:3 M	0.08	128.0 ± 10.8	6.1	7.7
BC D 8	7		0.04	119.7 ± 11.2	6.2	7.9
BC D 9	8	1:30 M	0.02	127.0 ± 10.7	5.9	7.2
BC D10	7		0.01	118.0 ± 11.2	6.0	7.3

From the table it is evident that though the varying type and number of constraints do not change significantly, the quality of the co-ordinates in the seven baseline solutions (D2, D8, D10) is better, as the adjusted lengths agree better with their measured values, than in the eight-baseline solutions (D12, D7, D9). It is also seen that the inclusion of the single east-west Australian line increases the semi-diameter by the unreasonable amount of 6 - 9 m (1 - 1.5 parts per million) in all cases.

On the basis of the results in tables 4 to 6 and also based on other calculations not reported here, the measured value of the Australian line 6032 - 6060 was rejected as a useful constraint.

The high standard deviations attached to the semi-diameters of the level ellipsoids in table 6 also indicates the questionable value of only seven or eight baselines in scaling a global network regardless of their individual quality. The inclusion of height constraints in the solution is an attempt for a better scale.

3.3 Use of Constrained Ellipsoidal Heights as Scalars

The use of geodetic (ellipsoidal) heights as weighted constraints as a contribution to the scale requires a more detailed explanation (figure 2). The height H above a geocentric reference ellipsoid

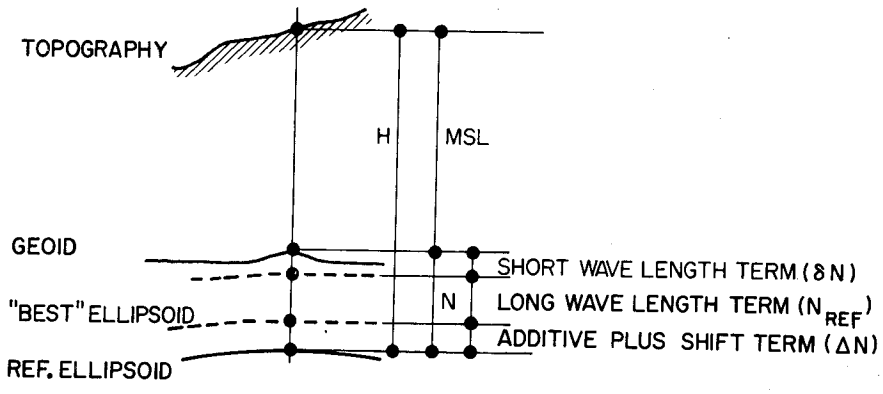

Figure 2. Height Components

has two main components:

- the orthometric (mean sea level) height (MSL); and
- the geoid undulation (N).

In this geocentric case, N consists of a long-wavelength component N_{REF}, a short-wavelength term δN, and an additive part Δa. The term N_{REF} generally corresponds to regional gravitational effects and can be computed for example from a truncated spherical harmonic series. The short-wavelength part δN corresponds to local gravity or mass disturbances and is generally not contained in the spherical harmonic representation. The additive part Δa is the so-called zero degree term which may exist due to the fact that the ellipsoid may not be of the same size (though it is of the same flattening) as the "best" (mean Earth) *level ellipsoid* to which the undulation N_{REF} is referenced. Since the N_{REF} undulations are, within reasonable limits, insensitive to the semi-diameter of the level ellipsoid, it is difficult to define a correct value for Δa. If the reference ellipsoid is *non-geocentric*, as is the case in this solution, an additional height term dH arises due to the "shift" of the origin (ellipsoidal centre) with respect to the geocentre. Thus the geodetic height may have the following components:

$$H = MSL + N \tag{1}$$

and

$$N = N_{REF} + \delta N + \Delta N \tag{2},$$

where (HEISKANEN & MORITZ 1967,p.207)

$$\Delta N = \Delta a + dH = \Delta a + u_o \cos\phi \cos\lambda + v_o \cos\phi \sin\lambda + w_o \sin\phi \tag{3},$$

Δa = a(level ellipsoid) - a(reference ellipsoid),

u_o, v_o, w_o are the co-ordinates of the geocentre with respect to the centre of the reference ellipsoid (origin); and

ϕ, λ are the geodetic co-ordinates of the station to which H refers.

In practice, at most satellite tracking stations, the quantity $MSL+N_{REF}$ is well known, and generally it constitutes the largest portion of the total height above the level ellipsoid. The additive plus shift term ΔN can be determined empirically through an iterative interpolation procedure as described later. Since $(MSL + N_{REF} + \Delta N)$ constitute the largest portion of the total height above the *reference ellipsoid* , it seems reasonable not to ignore this, admittedly partial, information on the height of the station and to include it in the adjustment as a constraint $(H_{CONSTR} = MSL + N_{REF} + \Delta N)$ with such a weight that the adjustment should be able to "pull out" the only remaining component, the short-wavelength term δN, together with possible errors in H_{CONSTR}. In this solution, the standard deviations used in computing the weights vary from ±2.5 m to ±8 m depending mostly on the location of the station, from the point of view of the extent of the available surface gravity observations in the area which was included in the spherical harmonic expansion for N_{REF} (RAPP 1973).

In trying to determine the "best" scale for the solution or, which is the same, the "best" additive term Δa, the first step is to establish the relationship between them. The problem differently stated is the determination of the relationship between the additive term and the semi-diameter of the "best" level ellipsoid to which the quantity N_{REF} refers. The meaning of the term "best" will be elaborated on later in this section. This is accomplished empirically from a set of solutions with height constraints containing different additive terms, from Δa = 0 to 30 m. The shift term dH initially is estimated from comparisons with various dynamic solutions, resulting in the

co-ordinates u_o, v_o and w_o needed in equation 3. These solutions result in sets of geodetic heights (H_{WNi}) above the reference ellipsoid and also in sets of undulations after subtracting the MSL:

$$N_{WNi} = H_{WNi} - MSL.$$

These undulations thus refer to the reference ellipsoid of a = 6 378 155 m, whose origin is set by the inner constraint. Disregarding the short-wavelength term, the relationship between the undulations N_{WNi} and N_{REF} is given by equations 2 and 3, from where, for any station and for the solution WNi:

$$(N_{WNi} - N_{REF}) - (\Delta a_i + u_{oi}\cos\phi\cos\lambda + v_{oi}\cos\phi\sin\lambda + w_{oi}\sin\phi) = 0.$$

Since the quantity $(N_{WNi} - N_{REF})$ is known at all stations, the parameters Δa_i, u_{oi}, v_{oi}, w_{oi} can be calculated (iterated) from least squares adjustments for each set "i". This is the same as determining the size (scale) and the origin of the level ellipsoid which fits best the geoid defined for a given set by the undulations N_{WNi}. Its size is

$$a_i = 6\,378\,155 + \Delta a_i$$

and its origin with respect to the origin of the reference ellipsoid is defined by the co-ordinates u_{oi}, v_{oi} and w_{oi}. After some iterations, these co-ordinates hardly change from solution (set) to solution (set), regardless of the initial selection of Δa; thus the relationship between the input additive term and the resulting semi-diameter, $a = f(\Delta a)$, becomes straightforward and linear.

This empirically determined relationship is shown in figure 3, as the dashed line drawn from the lower left corner towards the upper right. The corresponding ordinate is on the right hand side of the diagram. The line now allows either to pick the correct initial additive term which when used in the height constraints, would result in an a priori defined semi-diameter (scale), or to determine which semi-diameter (scale) would correspond to an a priori defined additive term. As an example, if the semi-diameter of the level ellipsoid best fitting the geoid was to be 6 378 142 m, the WN solution would require height constraints computed with an additive term of -15 m.

The next question, of course, is just how big should this desired semi-diameter be. Putting it differently, what criterion should be used to select the "best" scale ? If the scale was to be determined only from the EDM and C-Band baselines and/or the SECOR observations, these questions would not arise since the scale would be inherently defined. The use of weighted height constraints, as explained above, provides a unique tool to select the scale to fit some criterion. There could be several non-inclusive criteria, e.g.,

(1) The lengths of the EDM baselines as computed from the adjusted co-ordinates of the terminal stations should be
   - (a) exactly the same as the given lengths in table 3, or
   - (b) their differences should be within the limit of one (average) standard deviation,

   or (c) within a certain limit, e.g., 1:1,000,000, etc.

(2) Same as (1) but for the C-Band baselines.

(3) The scale difference as determined from the station co-ordinates of the WN solution and from the same co-ordinates of *some* dynamic solution should be
   - (a) exactly zero,
   - (b) within the limit of one standard deviation of the scale difference factor,
   - (c) within 1:1,000,000, etc.

(4) The scale difference as determined in (3) should be within a certain limit with respect to *all* the dynamic solutions.

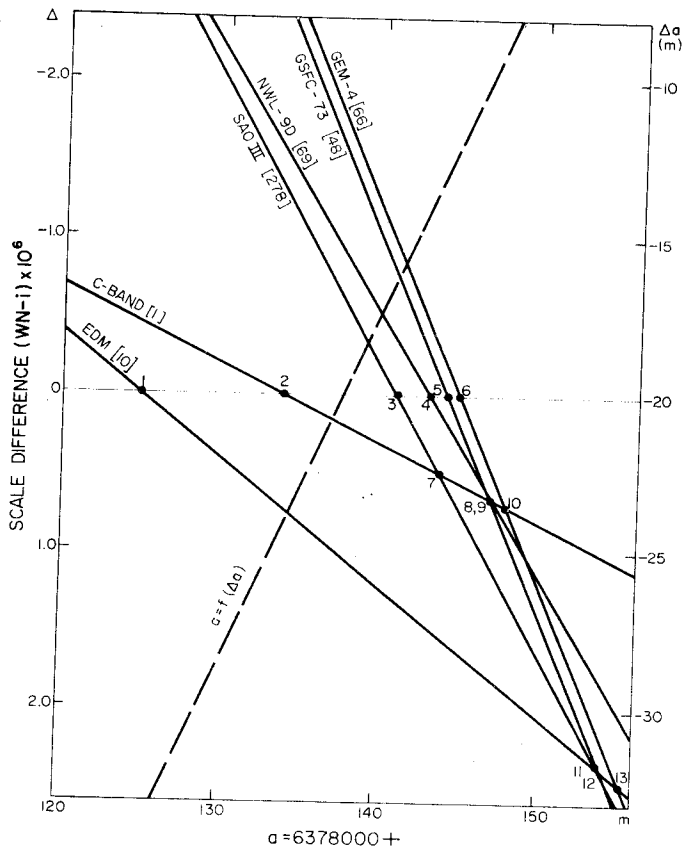

Figure 3. Determination of Scale

(5) The scale difference should be within a certain limit with respect to all the dynamic solutions *and* the EDM and C-Band baselines.

In order to be able to enforce any of the above criteria, first the relationship between the scale difference factor and the semi-diameter has to be established. This is accomplished again empirically by determining the scale differences between the different WNi solutions (used to determine the function a = f(Δa)) and the EDM and C-Band baselines and the dynamic solutions NWL-9D (ANDERLE 1973), SAO III (GAPOSCHKIN ET AL 1973), GEM 4(LERCH ET AL 1972), GSFC 73 (MARSH ET AL 1973). The method of calculating the scale difference factor is described in (KUMAR 1972), and the results are shown in figure 3 where, with the ordinate on the left hand side, the scale differences are plotted against the semi-diameters corresponding to the various Δa's used in the height constraints. The numbers on the lines indicate relative weights based on the uncertainties of the scale-difference determinations. It can be seen that the lines representing the geometric (EDM and C-Band) scale differences are much less well determined than the dynamic ones. As an example, the scale-difference factor between the WNi solution computed with Δa = -15 m (a = 6 378 142 m), and the solutions NWL-9D is -0.18×10^{-6}; the GEM 4 is -0.68×10^{-6} (the dynamic scales are larger). Also, the lengths of the EDM baselines from the adjustment differ from their directly measured values by 1.38×10^{-6} (the measured values are smaller).

The diagram is used by recognizing the importance of the various intersection points, marked by numbers. For example, point 1 illustrates the fact that if the semi-diameter of the level ellipsoid

was 6 378 125 m, the difference between the adjusted chord lengths and their given values would be zero; point 4 shows that with an a = 6 378 143 m, there would be no scale difference between WNi and NWL-9D. Fourteen similar intersection points are listed in table 7 with weights and interpretation.

From the table it is immediately clear that taking the weighted mean of the intersection points from the "geometric" scalars (points 1 and 2), the "best" semi-diameter is 6 378 125.8 m, while from the "dynamic" lines (points 3 - 6) it is 6 378 142.0 m. The difference of some 16 m, or about 2.5 parts in a million, seems to be real but unexplained at this time. The combined weighted mean from points 1 - 6 is 6 378 141.7 m; while from all the points (1 - 14), it is 6 378 142.7 m.

For the solution reported here (WN14), the criterion for the scale is (5) above; i.e., that the scale should correspond well to all geometric and dynamic information available at present. Based on the above numbers and on previously published parameters, a = 6 378 142 m was *selected*. This then requires an adjustment in which the scale is defined, in addition to the SECOR, EDM and C-Band observations, through height constraints with the initial additive constant $\Delta a = -15$ m. As can be seen from figure 3, at this semi-diameter, the maximum scale difference expected between WN14 and any of the dynamic solutions is about 0.8×10^{-6}, and with respect to the EDM about 1.4×10^{-6} or 1:700,000 which is about the average standard deviation of the EDM baselines. Using this scale, the resulting geoid undulations

$$N = H_{WN14} - MSL - \Delta N \qquad (4),$$

with

$$\Delta N(\text{metres}) = -13 - 23.2 \cos\phi \cos\lambda - 2.9 \cos\phi \sin\lambda + 2.7 \sin\phi$$

Table 7

Determination of Scale

Point	Interpretation	Weight	a (m)	Weighted Mean a (m)
1	WN = EDM	10	6 378 125.0	6 378 125.8 (from points 1 & 2)
2	WN = C-Band	1	6 378 133.7	
3	WN = SAO III	278	6 378 140.8	6 378 141.7 (from points 1 - 6)
4	WN = NWL 9D	69	6 378 143.0	
5	WN = GSFC 73	66	6 378 144.9	6 378 142.0 (from points 3 - 6)
6	WN = GEM 4	48	6 378 144.1	
7	C-Band = SAO III	1	6 378 143.6	6 378 142.7 (from points 1 - 14)
8	C-Band = GSFC 73	1	6 378 146.8	
9	C-Band = NWL 9D	1	6 378 147.1	
10	C-Band = GEM 4	1	6 378 147.8	
11	EDM = SAO III	10	6 378 153.7	
12	EDM = GSFC 73	8	6 378 154.0	
13	EDM = GEM 4	9	6 378 155.2	
14	EDM = NWL 9D	9	6 378 160.5	

are consistent with dynamically computed ones when the following set of constants defining the gravity of the level ellipsoid are used (HEISKANEN & MORITZ 1967, p.64):

$f = 1/298.25$ (flattening) ; $\omega = 0.729\,211\,514\,67 \times 10^{-4}$ sec^{-1} (rotational velocity);

$a = 6\,378\,142$ m ; and

$W_o = 6\,263\,688.00$ kgal m (geopotential on the geoid).

Derived from these are the following parameters:

$k^2M = 3.986\,009\,22 \times 10^{14}$ m^{3}sec^{-1} (gravitational constant × Earth mass);

$\gamma_e = 978.032\,26$ cm sec^{-2} (equatorial normal gravity); and

$J_2 = 1\,082.6863 \times 10^{-6}$ (second degree harmonic).

All the above constants are in good agreement with their current best estimates. The parameters in equation 4 ($\Delta a = -13 \pm 0.7$ m, $u_o = -23.2 \pm 0.9$ m, $v_o = -2.9 \pm 0.8$ m, $w_o = 2.7 \pm 1.2$ m) are the result of fitting an ellipsoid to the WN14 geoid as explained earlier in this section, and they represent the size and position of the best fitting level ellipsoid with respect to the reference ellipsoid (of the same flattening). In the case of a good global station distribution, the centre of this level ellipsoid is the "geometric" centre of the geoid. If this point is assumed to be identical with the centre of mass, then the above co-ordinates may be viewed as its co-ordinates with respect to the origin of the reference ellipsoid, and with opposite signs they can be used to shift the WN14 co-ordinates to the geocentre:

$$\begin{aligned} u(\text{geocentric}) &= u_{WN14} + 23.2 \text{ m} \\ v(\text{geocentric}) &= v_{WN14} + 2.9 \text{ m} \\ w(\text{geocentric}) &= w_{WN14} - 2.7 \text{ m} \end{aligned} \qquad (5).$$

It should be pointed out again that the selection of the semi-diameter 6 378 142 m was arbitrary. Had the lowest extremity in table 7 been chosen (6 378 125 m), the gravitational parameters (keeping f, ω and the geoidal undulations the same) still would not become completely unreasonable:

$W_o = 6\,263\,705.35$ kgal m ; $k^2M = 3.986\,009\,68 \times 10^{14}$ m^{3}sec^{-1}

$\gamma_e = 978.037\,62$ cm sec^{-2} ; $J_2 = 1\,082.695\,6 \times 10^{-6}$.

Thus the question of what is the "best" semi-diameter still needs to be answered.

4. Comparison of the Results

4.1 Comparisons with Geometric Information

In addition to solution WN14, two other adjustments were also performed with the same data. The only differences were that in one of them (WN12), the weighted height constraints were not applied; thus the scale is defined through the SECOR, EDM and C-Band data. In the other (WN16), the EDM and C-Band lengths were not entered as weighted constraints; thus the scale is through the SECOR and the weighted height constraints.

Table 8 contains differences between the adjusted and given chord lengths (table 3) from the three solutions. The lines originating from Station 4742 (Kauai) are not listed for reasons explained earlier. Comparing solutions WN14 and WN12, the effect of including the heights is not very significant. The average length discrepancy decreases 0.48×10^{-6} in the case of EDM, and 0.60×10^{-6} in the C-Band case, both numbers being within the noise level. At first glance, the difference between WN14 and WN16 seems to be significant since the average length discrepancy increases by about

Table 8

Chord Length Comparisons (Solutions WN12, 14 and 16)

Type	Line	Adjusted - Given Length					
		WN12		WN14		WN16	
		m	ppm	m	ppm	m	ppm
EDM	6002 - 6003	8.3 ± 2.5	2.38	2.7 ± 2.3	0.78	5.9 ± 3.0	1.70
	6003 - 6111	2.7 ± 1.4	1.90	2.3 ± 1.4	1.60	11.4 ± 3.1	8.00
	6006 - 6065	7.7 ± 2.1	3.13	6.1 ± 2.0	2.47	19.9 ± 3.5	8.13
	6016 - 6065	-2.8 ± 1.3	2.30	-2.9 ± 1.3	2.47	-18.9 ± 3.4	15.87
	6006 - 6016	2.7 ± 2.2	0.77	1.3 ± 2.1	0.37	1.6 ± 3.3	0.46
	6063 - 6064	13.7 ± 2.4	3.94	10.6 ± 2.3	3.03	15.2 ± 2.8	4.37
	6023 - 6060	7.9 ± 3.1	3.42	5.9 ± 3.0	2.55	9.6 ± 3.8	4.16
	6032 - 6060*	-2.4 ± 3.9	0.76	-4.5 ± 3.6	1.42	-2.9 ± 3.7	0.92
	3861 - 7043	2.2 ± 1.8	1.44	1.5 ± 1.8	0.99	7.6 ± 3.7	5.00
C-Band	4082 - 4050*	26.5 ± 6.9	2.42	-5.2 ± 3.9	0.48	-4.2 ± 4.0	0.39
	4082 - 4740	2.0 ± 2.7	1.25	1.3 ± 2.7	1.90	6.6 ± 5.0	4.13
	4082 - 4081	3.0 ± 2.3	2.40	2.3 ± 2.3	0.79	17.9 ± 6.2	14.49
	4082 - 4061	-0.4 ± 3.6	0.19	-1.5 ± 3.6	0.65	2.1 ± 6.1	0.93
Average	EDM		2.22		1.74		5.40
	C-Band		1.56		0.96		4.98
	All		2.02		1.50		5.27

4×10^{-6} or 1:250,000 for both types of observations. Close inspection, however, reveals that though the inclusion of the EDM and C-Band chords in the solution improves the positions of stations 6111 (Wrightwood), 6065 (H.Peissenberg) and 4081 (Grand Turk), it does not otherwise contribute to the overall scale determination significantly. If the above mentioned stations are left out of the comparison, the average length discrepancies in the WN16 solution decrease to 2.76×10^{-6} for the EDM and 1.81×10^{-6} for the C-Band, both within the noise level from WN14 (about 1×10^{-6}).

The above conclusion is also strengthened by the content of table 9 where the average standard deviations of the co-ordinates and the heights are compared from the three solutions. It is seen that while the inclusion of the weighted heights decreases standard deviations significantly, the exclusion of the geometric scalars hardly changes the results.

Table 9

Standard Deviation Comparisons
(Solutions WN12, 14 and 16)

Solution	Constituent Networks								WN_i	
	BC		SECOR		MPS		SA			
	σ	σ_H	σ	σ_H	σ	σ_H	σ	σ_H	σ	σ_H
WN12	4.4	5.0	4.2	4.8	6.9	7.6	5.2	5.9	5.5	6.2
WN14	3.5	3.2	2.8	2.4	4.8	2.9	4.1	3.0	3.9	2.9
WN16	3.5	3.2	2.8	2.4	4.9	2.9	4.1	3.0	4.0	2.9

All units in metres

4.2 Comparisons with Dynamic Solutions

Table 10 is a compilation of transformation parameters between the WN co-ordinates and those from the dynamic solutions NWL-9D, SAO III, GEM-4 and GSFC-73. The method of computing the parameters is described in (KUMAR 1972). In the table the positive angles ω, ψ and ε are counter-clockwise rotations about the w, v and u axes respectively, as viewed from the end of the positive axis. The scale difference factor Δ is in units of ppM. In the transformations the variances of both sets of the co-ordinates are taken into account. Taking the variances of the WN solutions as standard, those of the dynamic solutions are scaled by the weight factors indicated. These numbers are also indicative of the over-optimism over the quality of some of the published solutions. For example, a weight factor of 25 would indicate that the published standard deviations of a given solution need to be multiplied by $\sqrt{25} = 5$.

T a b l e 10

Relationships Between Various Dynamic and the WN Systems

(Dynamic - WN14)

Solution	NWL-9D			SAO III			GEM-4	GSFC-73
Sta. Considered	5000	6000	all	6000	9000	all	all	all
No. Stations	12	22	32	47	22	73	30	26
Weight Factor*	1.5	7.75	4	2	2	2	50	22
Δu(m)	15.6 ±1.6	16.8 ±1.1	15.9 ±1.0	16.8 ±1.5	10.7 ±2.1	13.9 ±1.3	14.5 ±1.6	13.7 ±1.5
Δv(m)	13.1 ±1.5	9.6 ±1.1	10.3 ±1.0	12.8 ±1.5	13.6 ±2.2	13.6 ±1.3	11.6 ±1.6	12.9 ±1.4
Δw(m)	-7.8 ±2.0	-3.2 ±1.1	-3.4 ±1.1	-5.2 ±1.5	-15.7 ±2.3	-10.4 ±1.3	1.9 ±1.7	-1.7 ±1.9
Δ (10^{-6})	0.74±0.15	0.26±0.05	0.29±0.04	-0.50±0.05	0.74±0.15	-0.17±0.04	0.93±0.11	0.96±0.11
ω ('')	0.73±0.03	0.70±0.01	0.71±0.01	0.51±0.02	0.26±0.03	0.37±0.01	-0.02±0.02	-0.38±0.02
ψ ('')	-0.11±0.04	-0.15±0.01	-0.15±0.01	0.15±0.02	0.08±0.04	0.15±0.01	0.12±0.03	0.19±0.03
ε ('')	0.23±0.07	-0.17±0.01	-0.14±0.01	-0.18±0.02	0.07±0.03	-0.03±0.01	0.17±0.02	0.24±0.03
σ_o^2	0.65	0.91	0.87	0.83	1.20	1.14	1.11	1.09

* Weight Factor = $\sigma_{o,i}^2 / \sigma_{o,WN14}^2$

As it is seen there is good agreement between the translational elements Δu-s and Δv-s of the main (all stations inclusive) dynamic solutions and a discrepancy of about 8.5 ± 1.7 m with respect to the geometric values (see equation 5). The largest discrepancy occurs in the Δw components, where there seems to be a 12.3 ± 2.1 m difference between the SAO III and the GEM-4 solutions. Eliminating the SAO III value, all Δw's, including the geometric one, are within the noise level.

The weighted mean shifts from the main dynamic solutions (excluding Δw from SAO III), or the co-ordinates of the geocentre with respect to the WN14 origin, are listed in table 11. The quantity $r_o = \sqrt{u_o^2 + v_o^2}$ is the distance of the WN14 origin from the rotation axis of the Earth. Calculating the same number from the JPL-LS 37 co-ordinates of the Deep Space Network (stations DSN1 = 4711, DSN2 = 4712, DSN4 = 4714, DSN6 = 4742 and DSN7 = 4751) as published in (GAPOSCHKIN ET AL 1973), one gets r_o = 25.9 ± 2.5 m, which value is nearest to the one calculated from the geometric fit.

The differences in scale between dynamic solutions are significant (see figure 3 for comparison). The largest discrepancy is between the SAOIII and GSFC-73 with $\Delta = (1.13 \pm 0.12) \times 10^{-6}$, which is

Table 11

Shifts to the Geocentre (Solution WN14)

Source	u_o (m)	v_o (m)	w_o (m)	r_o (m)
1. Dynamic Comparison	14.8 ± 1.4	11.8 ± 1.3	-1.8 ± 1.6	18.9 ± 1.9
2. Geometric Fit (eqn.5)	23.2 ± 0.9	2.9 ± 0.8	-2.7 ± 1.2	23.4 ± 1.2
3. Weighted Mean of 1 & 2	20.7 ± 1.2	5.3 ± 1.1	-2.4 ± 1.4	21.4 ± 1.6
4. JPL/DSN				25.9 ± 2.5

larger than what one would expect from the noise. The other dynamic scales are within near noise level and, on the average, differ from the scale of the WN14 solution by

$$\Delta = (0.12 \pm 0.08) \times 10^{-6}$$

or about one part in 8.3 million. The largest discrepancies occur in the orientation of the various dynamic systems with respect to each other and to WN14. In the rotation about the w axis (ω), the largest difference occurs between the NWL-9D and the GSFC-73 solutions, where $\omega = 1''.1$, or about 34 m on the equator (figure 4). The other differences are smaller but significant. These rotations may be partly due to the definition of the zero meridian in the case of purely electronic systems (e.g., Doppler), partly to the various definitions of vernal equinox in the star catalogues used, and also to its motion with respect to inertial space, in the case of optical observations. The latter alone requires a correction to the FK4 right ascensions amounting to $+0''.65$ at 1960.0, changing with a rate of $+1''.36$ per century (MARTIN & VAN FLANDERN 1970).

The rotations about the axes u and v are even more confusing. Figure 5 illustrates the situation at the pole. The weighted means of the dynamic solutions are $\psi = 0''.02 \pm 0''.02$ and $\varepsilon = -0''.04 \pm 0''.02$. The discrepancy between the poles as determined separately from the SAO III 6000 stations and then from the 9000 stations is unexplained at this time. It is interesting to note that the weighted mean pole and zero meridian positions computed from the dynamic solutions hardly differ from those of the WN14 solution.

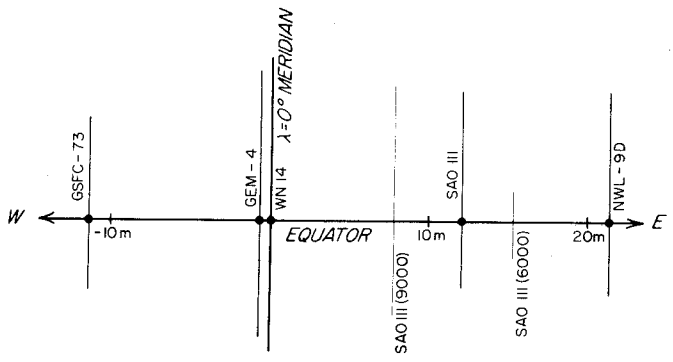

Figure 4. Dynamic Zero Meridians Relative to the WN14 Zero Meridian

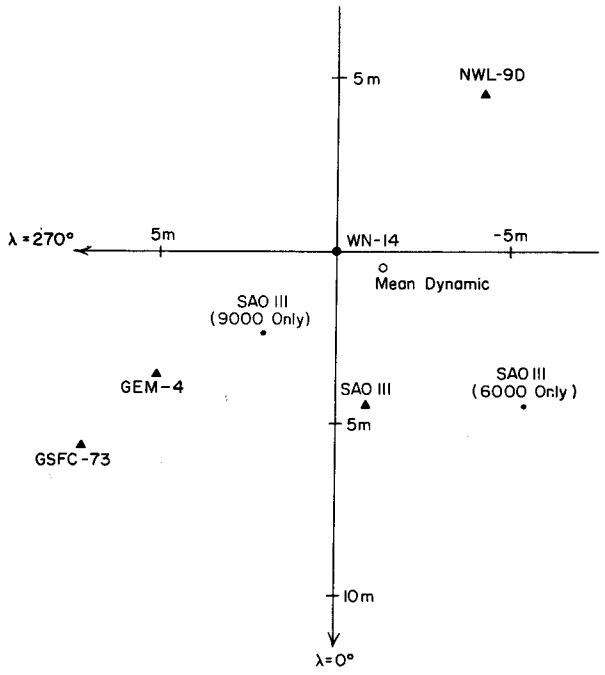

Figure 5. Dynamic Pole Positions Relative to the WN14 Pole

The only general conclusion that one can draw from the rotation parameters is that the co-ordinate systems used in the dynamic solutions need to be more carefully defined and conditions enforcing these definitions more strongly applied than evidenced from the solutions discussed.

4.3 Comparison with Geodetic Datums

Table 12 is a summary of datums. Table 13 summarizes the relationships between the various geodetic datums and the WN14 system for those datums where stations were located.

5. Cartesian Co-ordinates From Solutions WN12 and WN14

Table 14 is a summary of the Cartesian co-ordinates of solutions WN12 and WN14. As mentioned earlier the former differs from the latter only in that in it, the heights are not constrained. The resulting scale in WN12 is such that when the co-ordinates are transformed to a geocentric rotational ellipsoid of $a = 6\ 378\ 154$ m and $1/f = 298.2495$, they produce geoid undulations consistent with dynamically determined ones with $k^2M = 3.986\ 008\ 91 \times 10^{14} m^3 sec^{-2}$ and $\gamma_e = 978.028\ 47$ cm sec^{-2}. Derived from these constants are the values $W_o = 6\ 263\ 675.76$ kgal m and $J_2 = 1\ 082.6797 \times 10^{-6}$. These values together with those mentioned at the end of section 3.3 seem to be the extreme limits within which the truce must lie, provided that the dynamically determined undulations are correct.

Comparisons with geoid undulations from satellite and surface gravimetric solutions in case of the WN14 solution show an rms residual of ±6.1 m, with an average of only -0.3m. Similar comparison with the WN12 solution, where the heights are not constrained, shows that the rms of the residuals is ±16.1 m, and the average -0.2 m.

Table 12

Geodetic Datums

Code	Datum	Ellipsoid	Origin	Latitude	Longitude
1	Adindan (Ethiopia)	Clarke 1880	STATION Z5 ADINDAN	22°10'07".110	31°29'21".608
2	American Samoa 1962	Clarke 1866	BETTY 13 ECC	-14 20 08.341	189 17 07.750
3	Arc-Cape (South Africa)	Clarke 1880	Buffelsfontein	-33 59 32.000	25 30 44.622
4	Argentine	International	Campo Inchauspe	-35 58 17	297 49 48
5	Ascension Island 1958	International	Mean of three stations	-07 57	345 37
6	Australian Geodetic	Australian National	Johnston Memorial Cairn	-25 56 54.55	133 12 30.08
7	Bermuda 1957	Clarke 1866	FT. GEORGE B 1937	32 22 44.360	295 19 01.890
8	Berne 1898	Bessel	Berne Observatory	46 57 08.660	07 26 22.335
9	Betio Island, 1966	International	1966 SECOR ASTRO	01 21 42.03	172 55 47.90
10	Camp Area Astro 1961-62 USGS	International	CAMP AREA ASTRO	-77 50 52.521	166 40 13.753
11	Canton Astro 1966	International	1966 CANTON SECOR ASTRO	-02 46 28.99	188 16 43.47
12	Christmas Island Astro 1967	International	SAT.TRI.STA. 059 RM3	02 00 35.91	202 35 21.82
13	Chua Astro (Brazil-Geodetic)	International	CHUA	-19 45 41.16	311 53 52.44
14	Corrego Alegre (Brazil-Mapping)	International	CORREGO ALEGRE	-19 50 15.140	311 02 17.250
15	Easter Island 1967 Astro	International	SATRIG RM No. 1	-27 10 39.95	250 34 16.81
16	European	International	Helmert Tower	52 22 51.45	13 03 58.74
17	Graciosa Island (Azores)	International	SW BASE	39 03 54.934	331 57 36.118
18	Gizo, Provisional DOS	International	GUX 1	-09 27 05.272	159 58 31.752
19	Guam	Clarke 1866	TOGCHA LEE NO. 7	13 22 38.49	144 45 51.56
20	Heard Astro 1969	International	INTSATRIG 0044 ASTRO	-53 01 11.68	73 23 22.64
21	Iben Astro, Navy 1947 (Truk)	Clarke 1866	IBEN ASTRO	07 29 13.05	151 49 44.42
22	Indian	Everest	Kalianpur	24 07 11.26	77 39 17.57
23	Isla Socorro Astro	Clarke 1866	Station 038	18 43 44.93	249 02 39.28
24	Johnston Island 1961	International	JOHNSTON ISLAND 1961	16 44 49.729	190 29 04.781
25	Kusaie, Astro 1962, 1965	International	ALLEN SODANO LIGHT	05 21 48.80	162 58 03.28
26	Luzon 1911 (Philippines)	Clarke 1866	BALANCAN	13 33 41.000	121 52 03.000
27	Midway Astro 1961	International	MIDWAY ASTRO 1961	28 11 34.50	182 36 24.28
28	New Zealand 1949	International	PAPATAHI	-41 19 08.900	175 02 51.000
29	North American 1927	Clarke 1866	MEADES RANCH	39 13 26.686	261 27 29.494
30	*NAD 1927 (Cape Canaveral)	Clarke 1866	CENTRAL	28 29 32.364	279 25 21.230
31	*NAD 1927 (White Sands)	Clarke 1866	KENT 1909	32 30 27.079	253 31 01.306
32	Old Bavarian	Bessel	Munich	48 08 20.000	11 34 26.493
33	Old Hawaiian	Clarke 1866	OAHU WEST BASE	21 18 13.89	202 09 04.20
34	Ordnance Survey G.B. 1936	Airy	Herstmonceux	50 51 55.271	00 20 45.882
35	Pico de las Nieves (Canaries)	International	PICO DE LAS NIEVES	27 57 41.273	344 25 49.476
36	Pitcairn Island Astro	International	PITCAIRN ASTRO 1967	-25 04 06.97	229 53 12.17
37	Potsdam	Bessel	Helmert Tower	52 22 53.954	13 04 01.153
38	Provisional S.American 1956	International	LA CANOA	08 34 17.17	296 08 25.12
39	Provisional S. Chile 1963	International	HITO XVIII	-53 57 07.76	291 23 28.76
40	Pulkovo 1942	Krassovski	Pulkovo Observatory	59 46 18.55	30 19 42.09
41	South American 1969	South American 1969	CHUA	-19 45 41.653	311 53 55.936
42	Southeast Island (Mahe)	Clarke 1880		-04 40 39.460	55 32 00.166
43	South Georgia Astro	International	ISTS 061 ASTRO POINT 1968	-54 16 38.93	323 30 43.97
44	Swallow Islands (Solomons)	International	1966 SECOR ASTRO	-10 18 21.42	166 17 56.79
45	Tananarive	International	Tananarive Observatory	-18 55 02.10	47 33 06.75
46	Tokyo	Bessel	Tokyo Observatory (old)	35 39 17.51	139 44 40.50
47	Tristan Astro 1968	International	INTSATRIG 069 RM No. 2	-37 03 26.79	347 40 53.21
48	Viti Levu 1916 (Fiji)	Clarke 1880	MONAVATU (latitude only) SUVA (longitude only)	-17 53 28.285	178 25 35.835
49	Wake Island, Astronomic 1952	International	ASTRO 1952	19 17 19.991	166 38 46.294
50	Yof Astro 1967 (Dakar)	Clarke 1880	YOF ASTRO 1967	14 44 41.62	342 30 52.98
51	Palmer Astro 1969	International	ISTS 050	-64 46 35.71	295 56 39.53
52	Eftate	International	Belle Vue IGN	-17 44 17.400	168 20 33.250

*Local datums of special purpose, based on NAD 1927 values for the origin stations.

Table 13

Relationship Between Various Geodetic Datums and the WN System (Datum - WN14)

Datum No.	Datum Name[1]	No. of Stations	Δu (m)*	Δv (m)*	Δw (m)*	ω (″)**	ψ (″)**	ϵ (″)**	Δ (×10⁶)
1	Adindan (Ethiopia)	2	184 ±19	21 ±11	-200 ± 6				
2	American Samoa 1962	1	119 ± 8	-105 ± 8	-413 ±10				
3	Arc Cape (South Africa)	1	152 ± 7	126 ± 7	298 ±10				
5	Ascension Island 1958	1	227 ± 7	- 93 ± 7	- 58 ± 8				
6	Australian Geodetic	3	118.2± 5.0	41.1± 6.2	-121.0± 6.9	1.03±0.18	0.99±0.18	-0.25±0.22	-1.20±0.71
10	Camp Area Astro 1961/62(USGS)	1	111 ±10	148 ± 9	-238 ±10				
12	Christmas Island Astro 1967	1	-115 ± 9	-224 ±12	529 ± 8				
15	Easter Island Astro 1967	1	-182 ±10	-138 ±10	-128 ±11				
16	European-50 (W)[2]	11	133.3± 9.5	114.2±15.9	152.2± 9.2	-1.76±0.38	0.01±0.31	-0.38±0.44	-7.30±1.14
	European-50 (All stations)[3]	16	134.3± 9.1	152.7± 8.0	144.6± 8.8	-0.41±0.20	0.27±0.30	-0.51±0.22	-7.24±0.88
17	Graciosa Island (Azores)	1	123 ±17	-147 ± 9	37 ±17				
20	Heard Astro 1969	1	182 ±12	56 ±12	-114 ±14				
22	Indian[4]	1	-165 ±17	-711 ±10	-228 ±11				
23	Isla Socoro Astro	1	-134 ±12	-206 ± 7	-503 ± 9				
24	Johnston Island 1961	1	-161 ±13	51 ±25	211 ±13				
26	Luzon 1911 (Philippines)	1	151 ±10	51 ± 7	111 ± 8				
27	Midway Astro 1961	1	-377 ± 7	84 ± 7	-279 ± 9				

*If (Datum - Geocenter) is sought add to the tabulated values of Δu, Δv, Δw the respective quantities -21m, -5 m, 2 m see Table 11

**ω, ψ, ϵ when positive, represent counterclockwise rotations about the respective w, v, u axes, as viewed from the end of the positive axis.

Table 13 (cont'd)

Datum No.	Datum Name[1]	No. of Stations	Δu (m)*	Δv (m)*	Δw (m)*	ω(″)**	ψ(″)**	ε(″)	Δ(×10⁶)
28	New Zealand 1949	1	- 61 ± 8	41 ± 9	-192 ± 9				
29	North American 1927 (W)[5]	8	30.6± 7.3	-170.3± 4.5	-134.9± 6.8	0.21±0.20	0.59±0.21	-0.45±0.23	-7.91±0.45
	North American 1927 (E)[6]	13	56.4± 6.9	-144.6± 4.4	-196.4± 4.3	1.01±0.19	-0.01±0.16	0.54±0.14	2.15±0.62
	North American (All Stations)[7]	21	57.1± 2.2	-147.9± 2.6	-187.5± 2.9	0.86±0.06	0.23±0.06	0.33±0.11	0.80±0.27
36	Pitcairn Island Astro	1	-167 ±12	-168 ±11	- 60 ±11				
39	Provisional South Chile 1963	1	0 ± 8	-196 ± 8	- 93 ± 9				
41	South American 1969[9]	10	54.4± 5.5	30.0± 4.8	42.9± 4.9	-0.63±0.17	0.17±0.12	-0.12±0.13	6.67±0.59
42	Southeast Island (Mahe)	1	54 ± 8	186 ± 8	272 ± 9				
43	South Georgia Astro	1	820 ± 8	-101 ±11	291 ±11				
46	Tokyo	1	183 ±10	-506 ± 9	-686 ± 9				
47	Tristan Astro 1968	1	654 ±14	-420 ±11	622 ±13				
49	Wake Island Astronomic 1952	1	-260 ± 7	67 ±12	-140 ± 8				
50	Yof Astro 1967 (Dakar)	1	55 ± 6	-143 ± 7	- 95 ± 7				
51	Palmer Astro 1969	1	-218 ± 9	- 8 ±12	-226 ±12				

*If (Datum - Geocenter) is sought add to the tabulated values of Δu, Δv, Δw the respective quantities -21m, -5 m, 2 m see Table 11.

**ω, ψ, ε when positive, represent counterclockwise rotations about the respective w, v, u axes, as viewed from the end of the positive axis.

Table 13 (cont'd)

[1] See Table 12 for datum description and other related information.

[2] Stations included are Tromso (6006), Catania (6016), Hohenpeissenberg (6065), Wippolder (8009), Zimmerwald (8010), Haute Provence (8015), Nice (8019), Meudon (8030), San Fernando (9004), Dionysos (9091) and Harestua (9426).

[3] Stations included are as in #2 and Mashhad (6015), Malvern (8011), Naini Tal (9006), Shiraz (9008) and Riga (9431).

[4] Based on p. 70, Bulletin Geodesique, 107, 1973.

[5] Stations included are Goldstone (1030), Colorado Springs (3400), Vandenberg AFB (4280), Wrightwood II (6134), Moses Lake (6003), Edinburg (7036), Denver (7045) and Organ Pass (9001).

[6] Stations included are Blossom Point (1021), Fort Myers (1022), E. Grand Forks (1034), Rosman (1042), Bedford (3401), Semmes (3402), Hunter AFB (3648), Aberdeen (3657), Homestead (3861), Beltsville (6002), Greenbelt (7043), Jupiter (7072) and Sudbury (7075).

[7] Stations included are as in #4 and #5 above.

[8] Stations included are Brasilia (3414), Asunction (3431), Bogota (3477), Paramaribo (6008), Quito (6009), Villa Dolores (6019), Natal (6067), Arequipa (9007), Curacao (9009) and Comodoro Rivadavia (9031).

Table 14

Summary of Cartesian Coordinates (Solutions WN12 and WN14)

STATION		SOLUTION WN-12						SOLUTION WN-14					
NO	NAME	U	V	W	σ_u	σ_v	σ_w	U	V	W	σ_u	σ_v	σ_w
1021	BLOSSOM POINT	1118021.8	-4876331.7	3942970.9	3.1	4.0	4.2	1118023.1	-4876323.4	3942963.9	2.8	2.6	2.8
1022	FORT MYERS	807850.8	-5652004.0	2833509.0	2.6	3.3	3.3	807851.9	-5651989.6	2833500.2	2.2	1.9	2.3
1030	GOLDSTONE	-2357249.2	-4646346.4	3668312.5	6.1	4.4	4.7	-2357242.9	-4646338.5	3668306.8	5.6	3.3	3.2
1032	ST. JOHN'S	2602704.3	-3419179.7	4697621.1	49.1	89.5	29.9	2602688.6	-3419228.9	4697637.3	39.3	46.7	13.8
1033	FAIRBANKS	-2299292.3	-1445690.5	5751823.3	7.5	10.0	10.5	-2299282.6	-1445693.7	5751811.6	6.9	9.7	5.7
1034	E. GRAND FORKS	-521708.3	-4242074.9	4718726.5	3.5	4.0	4.4	-521704.5	-4242064.3	4718716.8	3.1	3.0	2.7
1042	ROSMAN	647495.9	-5177948.0	3656714.4	3.1	3.6	4.0	647497.5	-5177935.6	3656705.9	2.8	2.4	2.8
3106	ANTIGUA	2801840.5	-5372180.7	1868548.5	4.1	4.6	4.9	2801838.3	-5372164.6	1868538.6	3.7	3.3	4.3
3334	STONEVILLE	-84969.1	-5327986.3	3493434.3	15.6	14.0	10.8	-84963.8	-5327974.9	3493428.3	13.6	6.8	9.0
3400	COLORADO SPRINGS	-1275239.4	-4798062.9	3994229.5	16.3	12.4	8.6	-1275207.2	-4798029.3	3994208.3	9.1	5.1	5.7
3401	BEDFORD	1513134.8	-4463580.1	4283061.2	3.5	5.3	4.6	1513136.1	-4463576.8	4283055.8	3.2	3.4	3.0
3402	SEMMES	167256.1	-5481980.4	3245042.6	4.2	4.3	4.6	167259.7	-5481971.0	3245037.0	3.9	2.8	3.5
3404	SWAN ISLAND	642485.7	-6053942.4	1895690.5	5.0	5.3	5.5	642491.4	-6053940.3	1895688.6	4.7	3.7	4.9
3405	GRAND TURK	1919482.1	-5621096.5	2315780.1	3.6	5.6	4.9	1919482.9	-5621088.1	2315775.3	3.3	3.5	4.0
3406	CURACAO	2251802.9	-5816929.0	1327197.4	2.8	3.5	3.8	2251800.2	-5816912.9	1327191.1	2.4	2.1	3.4
3407	TRINIDAD	2979092.9	-5513532.6	1181126.8	5.2	5.1	5.9	2979091.1	-5513530.9	1181129.3	4.7	3.4	5.3
3413	NATAL	5186366.4	-3654225.1	-653022.7	3.4	2.9	3.2	5186348.4	-3654222.4	-653018.9	2.1	2.2	2.7
3414	BRASILIA	4114987.8	-4554148.5	-1732166.1	9.9	8.4	7.9	4114977.8	-4554142.5	-1732154.0	7.7	6.1	7.2
3431	ASUNCION	3093056.1	-4870100.4	-2710845.8	8.5	9.3	12.5	3093045.4	-4870081.7	-2710823.0	7.6	6.5	10.8
3476	PARAMARIBO	3623293.6	-5214213.7	601514.0	3.4	3.3	3.6	3623277.3	-5214210.7	601515.3	2.2	2.0	3.0
3477	BOGOTA	1744649.6	-6114305.6	532205.2	10.4	13.7	9.8	1744650.2	-6114296.7	532208.6	10.2	6.6	9.6
3478	MANAUS	3185705.4	-5514574.5	-347713.2	19.3	35.4	35.8	3185777.0	-5514585.9	-347703.2	18.7	14.5	35.1
3499	QUITO	1280834.0	-6250966.2	-10605.5	3.8	5.9	4.5	1280834.2	-6250955.9	-10600.6	3.6	3.4	4.1
3648	HUNTER AFB	832562.6	-5349553.4	3360596.4	4.1	5.0	5.4	832566.2	-5349540.7	3360585.3	3.6	2.5	3.6
3657	ABERDEEN	1186786.1	-4785205.1	4032892.3	3.4	5.0	4.5	1186787.1	-4785193.1	4032882.3	3.1	3.0	3.0
3661	HOMESTEAD	961766.7	-5679170.6	2729883.8	3.3	3.8	3.7	961767.9	-5679156.6	2729883.5	3.0	2.3	2.6
3902	CHEYENNE	-1234689.4	-4651235.9	4174763.4	28.6	32.1	11.3	-1234700.7	-4651242.8	4174758.6	8.6	6.3	6.3
3903	HERNDON	1088960.0	-4842973.2	3991763.9	12.3	15.5	11.4	1088989.7	-4843005.4	3991776.6	12.1	8.5	8.9
4050	PRETORIA	5051614.8	2726608.6	-2774181.0	4.4	3.8	5.5	5051608.1	2726603.3	-2774166.8	3.2	3.2	4.4
4061	ANTIGUA	2801594.5	-5372540.2	1868034.3	4.2	4.7	5.0	2801592.3	-5372523.9	1868024.4	3.8	3.5	4.3
4081	GRAND TURK	1920409.9	-5619426.1	2319133.4	3.7	5.7	5.0	1920410.9	-5619417.8	2319128.5	3.3	3.6	4.0
4082	MERRITT ISLAND	910567.9	-5539130.2	3017974.8	2.9	3.8	3.7	910567.2	-5539113.2	3017965.3	2.6	2.4	2.8
4280	VANDENBERG AFB	-2671883.7	-4521217.3	3607495.0	4.3	4.4	4.8	-2671873.8	-4521210.5	3607490.4	3.8	3.3	3.6
4740	BERMUDA	2308008.6	-4874314.8	3393092.0	3.8	5.4	5.1	2308007.3	-4874298.2	3393082.1	3.3	3.1	3.8
5001	HERNDON	1088874.4	-4842954.9	3991857.8	4.9	10.2	7.9	1088849.4	-4842948.7	3991840.2	3.6	3.0	3.7
5201	MOSES LAKE	-2127810.4	-3785912.3	4656011.9	2.7	2.8	3.7	-2127802.2	-3785911.5	4656012.1	2.3	2.2	2.4
5410	MIDWAY ISLANDS	-5618764.5	-250231.5	2997243.8	2.9	3.2	4.1	-5618754.1	-250237.5	2997250.2	2.3	2.8	3.6
5648	FORT STEWART	794687.3	-5360063.7	3353093.5	4.2	5.0	5.5	794691.0	-5360051.1	3353082.4	3.6	2.5	3.6
5712	PARAMARIBO	3623307.1	-5214190.5	601672.3	3.4	3.3	3.6	3623289.8	-5214188.0	601673.2	2.1	2.0	2.9
5713	TERCEIRA	4433654.4	-2268159.2	3971673.1	2.7	2.8	3.8	4433637.8	-2268153.2	3971656.8	2.0	2.2	2.5

Table 14 (cont'd)

STATION		SOLUTION WN-12						SOLUTION WN-14					
NO	NAME	U	V	W	σ_u	σ_v	σ_w	U	V	W	σ_u	σ_v	σ_w
5715	DAKAR	5084479.9	-1853580.1	1612763.8	2.3	2.5	3.1	5084468.8	-1853580.1	1612760.1	1.6	2.0	2.3
5717	FORT LAMY	6023416.1	1617949.5	1331651.2	2.7	2.8	3.3	6023410.7	1617946.5	1331655.8	2.0	2.0	2.7
5720	ADDIS ABADA	4900750.1	3968255.1	966348.3	2.7	2.9	3.4	4900749.1	3968253.0	966354.7	2.0	2.1	2.9
5721	MASHHAD	2604406.6	4444124.9	3750345.7	2.6	2.8	3.5	2604404.8	4444122.3	3750344.3	2.1	2.1	2.7
5722	DIEGO GARCIA	1905122.3	6032294.5	-810726.4	4.2	5.5	4.8	1905127.0	6032287.5	-810716.2	3.5	4.1	4.3
5723	CHIANG MAI	-941713.7	5967448.6	2039317.5	3.1	3.3	4.1	-941709.4	5967445.0	2039322.9	2.5	2.3	3.5
5726	ZAMBOANGA	-3361953.2	5365845.5	763623.6	3.0	3.3	3.8	-3361946.8	5365837.0	763627.8	2.3	2.2	3.2
5730	WAKE ISLAND	-5858583.8	1394474.9	2093844.7	2.8	3.1	3.8	-5858574.6	1394467.2	2093847.4	2.1	2.5	3.1
5732	PAGO PAGO	-6099984.0	-997345.6	-1568577.0	5.7	4.4	4.9	-6099970.5	-997355.3	-1568570.9	3.6	3.5	4.1
5733	CHRISTMAS ISLAND	-5885350.8	-2448375.3	221663.1	4.4	3.5	4.6	-5885333.9	-2448380.4	221670.7	2.7	2.9	3.9
5734	SHEMYA	-3851806.1	396416.1	5051343.3	3.2	3.7	4.9	-3851799.0	396409.3	5051342.0	2.7	3.3	3.9
5735	NATAL	5186368.5	-3654226.0	-653022.6	3.3	2.8	3.1	5186350.6	-3654223.7	-653018.9	2.0	2.1	2.5
5736	ASCENSION ISLAND	6118355.5	-1571763.1	-878558.4	3.3	2.9	3.3	6118340.3	-1571761.9	-878553.6	2.3	2.2	2.7
5739	TERCEIRA	4433646.0	-2268192.2	3971663.3	2.7	2.8	3.8	4433629.3	-2268186.2	3971647.0	2.0	2.2	2.5
5744	CATANIA	4896444.1	1316129.4	3856628.4	2.4	2.8	3.2	4896437.7	1316125.0	3856626.2	1.8	2.2	2.3
5907	WORTHINGTON	-449391.6	-4600910.6	4380315.4	5.8	13.8	13.5	-449417.5	-4600905.5	4380280.1	4.2	3.2	4.5
5911	BERMUDA	2308010.4	-4873778.3	3394476.1	3.6	4.9	5.2	2307991.2	-4873773.2	3394463.4	2.6	2.3	3.0
5912	PANAMA	1142664.4	-6196104.1	988340.8	4.8	9.1	7.0	1142644.5	-6196109.1	988336.6	3.1	3.4	4.1
5914	PUERTO RICO	2349423.9	-5576023.2	2010340.5	13.5	21.1	9.7	2349456.9	-5576027.1	2010342.6	10.5	7.0	6.4
5915	AUSTIN	-744066.7	-5465234.3	3192485.8	5.6	15.3	12.8	-744091.1	-5465238.7	3192467.4	3.8	3.8	4.7
5923	CYPRUS	4363335.9	2862258.8	3655280.7	2.5	2.7	3.3	4363332.2	2862254.9	3655280.7	1.9	2.1	2.4
5924	ROTA	5093565.8	-565319.1	3784273.1	2.4	3.1	3.8	5093556.2	-565322.3	3784268.3	1.9	2.6	2.9
5925	ROBERTS FIELD	6237376.8	-1140241.8	687740.0	3.0	3.1	3.6	6237366.3	-1140241.5	687740.2	2.3	2.6	3.0
5930	SINGAPORE	-1542556.4	6186964.6	151827.8	3.3	3.9	4.0	-1542549.4	6186956.7	151833.8	2.6	2.7	3.4
5931	HONG KONG	-2423919.1	5388254.8	2394863.9	3.1	3.5	4.3	-2423914.9	5388250.3	2394869.2	2.5	2.5	3.6
5933	DARWIN	-4071578.3	4714767.0	-1366533.3	4.3	4.4	4.3	-4071568.4	4714253.3	-1366528.3	3.2	3.2	3.7
5934	MANUS	-5367671.7	3437861.4	-225419.4	3.6	3.5	3.8	-5367663.1	3437869.9	-225416.0	2.5	2.5	3.3
5935	GUAM	-5059832.6	3591194.2	1472759.4	2.9	3.0	3.4	-5059825.7	3591186.0	1472762.5	2.1	2.2	2.8
5937	PALAU	-4433470.5	4512939.3	809955.3	3.1	3.2	3.7	-4433463.6	4512930.3	809958.7	2.2	2.2	3.2
5938	GUADALCANAL	-5915106.0	2146873.2	-1037912.8	4.4	3.9	4.0	-5915096.5	2146860.8	-1037909.5	3.0	3.0	3.5
5941	MAUI	-5467771.9	-2381242.7	2254024.0	3.5	3.2	4.4	-5467757.3	-2381246.7	2254033.8	2.5	2.8	3.8
6001	THULE	546566.4	-1389993.6	6180242.4	2.7	2.7	4.4	546568.7	-1389993.7	6180236.7	2.6	2.4	3.4
6002	BELTSVILLE	1130762.7	-4830837.6	3994709.9	2.2	2.7	3.1	1130764.9	-4830831.9	3994704.0	2.0	1.7	1.9
6003	MOSES LAKE	-2127839.9	-3785864.2	4656037.4	2.5	2.7	3.5	-2127832.1	-3785863.0	4656037.2	2.1	2.0	2.3
6004	SHEMYA	-3851806.8	396416.1	5051341.7	3.2	3.7	5.0	-3851797.5	396409.4	5051340.5	2.7	3.3	3.9
6006	TROMSO	2102930.3	721674.1	5958181.7	2.7	3.3	4.4	2102927.4	721660.5	5958180.8	2.4	2.9	2.9
6007	TERCEIRA	4433653.3	-2268156.9	3971671.0	2.7	2.7	3.8	4433637.3	-2268151.4	3971655.0	2.0	2.2	2.5
6008	PARAMARIBO	3623257.3	-5214236.7	601534.8	3.4	3.3	3.6	3623241.0	-5214233.7	601536.1	2.1	2.0	2.9
6009	QUITO	1280834.0	-6250966.2	-10805.5	3.8	5.9	4.5	1280834.2	-6250955.9	-10800.6	3.6	3.4	4.1
6011	MAUI	-5466039.2	-2404429.3	2242224.6	4.4	3.4	3.9	-5466018.6	-2404431.5	2242224.4	3.0	2.9	3.3

Table 14 (cont'd)

STATION		SOLUTION WN-12						SOLUTION WN-14					
NO	NAME	U	V	W	σ_u	σ_v	σ_w	U	V	W	σ_u	σ_v	σ_w
6012	WAKE ISLAND I	-5858578.8	1394516.4	2093817.4	2.9	3.2	3.8	-5858569.3	1394508.7	2093820.3	2.1	2.6	3.2
6013	KANOYA	-3565901.4	4120723.2	3303426.9	4.0	5.2	5.9	-3565892.8	4120713.6	3303428.3	3.3	4.4	4.9
6015	MASHHAD	2604355.4	4444169.2	3750321.7	2.6	2.9	3.5	2604353.3	4444166.0	3750320.5	2.1	2.2	2.6
6016	CATANIA	4896394.6	1316176.2	3856670.7	2.4	2.8	3.2	4896388.3	1316172.1	3856668.2	1.8	2.2	2.2
6019	VILLA DOLORES	2280630.7	-4914547.7	-3355417.9	2.7	3.6	5.2	2280627.1	-4914543.2	-3355402.8	2.4	2.7	3.7
6020	EASTER ISLAND	-1858621.5	-5354898.4	-2095762.3	6.0	6.1	6.9	-1858614.3	-5354894.4	-2095749.0	5.4	4.5	5.5
6022	TUTUILA	-6099975.9	-997357.7	-1568593.6	4.8	3.9	5.2	-6099961.7	-997362.2	-1568585.5	3.4	3.6	4.7
6023	THURSDAY ISLAND	-4955391.2	3842255.7	-1163855.5	4.5	3.9	4.7	-4955386.8	3842247.8	-1163847.4	3.2	3.0	4.0
6031	INVERCARGILL	-4313830.4	891340.6	-4597277.7	4.4	4.2	5.3	-4313825.3	891333.9	-4597265.8	3.4	3.9	3.8
6032	CAVERSHAM	-2375426.0	4875557.6	-3345424.5	3.7	4.3	5.0	-2375420.6	4875546.7	-3345411.1	3.3	3.2	3.9
6038	SOCORRO ISLAND	-2160989.6	-5642717.9	2035360.0	2.9	3.8	4.4	-2160980.9	-5642710.5	2035367.8	2.5	2.8	3.8
6039	PITCAIRN ISLAND	-3724775.0	-4421234.4	-2686094.4	7.9	7.2	7.3	-3724765.9	-4421237.6	-2686084.7	6.2	5.4	5.5
6040	COCOS ISLAND	-741986.1	6190803.6	-1330567.1	4.7	4.8	4.7	-741981.7	6190792.9	-1330546.3	4.5	3.7	4.2
6042	ADDIS ABABA	4900752.0	3968255.1	966318.9	2.7	2.9	3.4	4900750.7	3968252.7	966325.3	2.0	2.1	2.9
6043	CERRO SOMBRERO	1371376.5	-3614750.6	-5055947.1	3.5	4.2	7.0	1371375.9	-3614750.3	-5055927.8	3.3	3.8	4.8
6044	HEARD ISLAND	1098098.5	3684617.0	-5071900.1	6.9	6.7	11.1	1098097.9	3684606.6	-5071873.1	6.8	6.2	7.8
6045	MAURITIUS	3223434.7	5045343.6	-2191818.0	3.6	4.0	4.6	3223432.0	5045336.3	-2191805.7	3.2	3.1	3.9
6047	ZAMBOANGA	-3361983.5	5365820.6	763620.5	3.1	3.4	3.8	-3361976.9	5365811.9	763624.7	2.4	2.3	3.2
6050	PALMER STATION	1192679.3	-2451013.2	-5747052.4	5.0	6.3	9.8	1192678.8	-2451015.6	-5747034.2	4.9	6.1	6.1
6051	MAWSON STATION	1111337.1	2169270.2	-5874355.2	5.0	4.2	7.3	1111336.1	2169262.7	-5874334.1	4.9	3.7	4.4
6052	WILKES STATION	-902611.4	2409530.0	-5816569.9	4.6	4.4	7.4	-902608.8	2409522.1	-5816551.8	4.4	4.0	5.4
6053	MCMURDO STATION	-1310854.8	311262.9	-6213294.3	4.8	4.8	7.4	-1310852.3	311257.5	-6213276.5	4.6	4.5	4.3
6055	ASCENSION ISLAND	6118349.3	-1571749.2	-878601.3	3.3	2.9	3.4	6118334.2	-1571748.3	-878596.5	2.3	2.3	2.8
6059	CHRISTMAS ISLAND	-5885350.2	-2448374.4	221663.6	4.3	3.4	4.5	-5885333.5	-2448379.0	221671.1	2.7	2.9	3.8
6060	CULGOORA	-4751655.0	2792065.7	-3200174.2	4.5	4.0	4.7	-4751650.0	2792058.1	-3200164.0	3.3	3.3	3.7
6061	SOUTH GEORGIA IS.	2999921.2	-2219366.3	-5155267.1	3.9	5.9	7.8	2999915.6	-2219369.3	-5155246.0	3.7	5.7	5.3
6063	DAKAR	5084479.3	-1653496.4	1612858.7	2.4	2.6	3.2	5084467.4	-1653495.8	1612855.1	1.7	2.1	2.5
6064	FORT LAMY	6023394.4	1617934.2	1331731.7	3.3	3.1	3.7	6023386.7	1617931.9	1331733.2	2.7	2.6	3.2
6065	HOHENPEISSENBERG	4213570.2	820833.7	4702786.5	2.6	3.0	3.6	4213564.6	820830.0	4702784.4	2.0	2.4	2.3
6066	WAKE ISLAND II	-5858580.7	1394474.0	2093843.0	2.9	3.2	3.8	-5858571.2	1394466.4	2093846.0	2.1	2.6	3.2
6067	NATAL	5186415.0	-3653935.9	-654280.7	3.3	2.8	3.1	5186397.1	-3653933.3	-654276.9	2.1	2.2	2.6
6068	JOHANNESBURG	5084837.1	2670346.5	-2768109.3	4.2	3.5	5.3	5084830.4	2670341.2	-2768095.2	3.0	2.9	4.2
6069	TRISTAN DA CUNHA	4978430.9	-1086871.1	-3823187.7	8.3	6.6	10.4	4978421.7	-1086874.0	-3823167.8	6.5	6.4	8.1
6072	CHIANG MAI	-941707.8	5967462.5	2039307.4	5.9	5.1	4.9	-941702.1	5967455.1	2039311.6	5.7	4.0	4.3
6073	DIEGO GARCIA	1905134.3	6032292.0	-810742.3	3.7	4.8	4.7	1905134.1	6032282.4	-810732.7	3.4	3.7	4.2
6075	MAHE	3602824.5	5238240.2	-515957.7	4.2	4.6	4.5	3602820.6	5238240.7	-515948.3	3.8	3.6	4.0
6078	PORT VILA	-5952307.7	1231910.5	-1925983.7	19.9	9.4	16.6	-5952303.4	1231904.9	-1925972.5	9.7	8.0	12.4
6111	WRIGHTWOOD I	-2448862.8	-4667992.3	3582759.4	3.0	3.2	3.8	-2448853.3	-4667985.8	3582754.9	2.6	2.1	2.4
6123	POINT BARROW	-1881807.4	-812435.3	6019599.3	4.9	4.6	7.1	-1881799.4	-812439.0	6019590.7	4.6	4.4	4.5
6134	WRIGHTWOOD II	-2448916.5	-4668082.4	3582454.1	3.0	3.2	3.8	-2448907.0	-4668075.9	3582449.6	2.6	2.1	2.4

Table 14 (cont'd)

STATION		SOLUTION WN-12						SOLUTION WN-14					
NO	NAME	U	V	W	σ_u	σ_v	σ_w	U	V	W	σ_u	σ_v	σ_w
7036	EDINBURG	-828491.0	-5657486.5	2816825.5	3.8	3.9	4.0	-828487.0	-5657471.3	2816816.0	3.5	2.4	2.9
7037	COLUMBIA	-191294.8	-4967308.3	3903264.5	3.2	3.5	3.9	-191291.0	-4967293.9	3903252.6	2.9	2.2	2.4
7039	BERMUDA	2308214.8	-4873614.8	3394568.4	3.7	5.3	5.0	2308213.4	-4873598.3	3394558.5	3.3	3.1	3.6
7040	SAN JUAN	2465050.9	-5534945.5	1985522.2	4.0	4.4	4.7	2465049.5	-5534930.0	1985513.1	3.7	3.2	4.0
7043	GREENBELT	1130706.5	-4831337.2	3994141.4	2.2	2.7	3.1	1130708.6	-4831331.3	3994135.5	2.0	1.7	1.9
7045	DENVER	-1240475.1	-4760256.0	4048997.8	4.6	4.2	4.7	-1240470.2	-4760242.1	4048985.3	4.2	2.8	2.9
7072	JUPITER	976261.3	-5601416.4	2880251.4	2.5	3.3	3.3	976261.3	-5601399.9	2880241.9	2.2	1.8	2.3
7075	SUDBURY	692618.7	-4347090.4	4600487.7	4.0	5.7	5.4	692620.7	-4347076.5	4600475.4	3.7	3.8	3.4
7076	KINGSTON	1384159.2	-5905680.0	1966554.4	4.3	5.8	5.9	1384158.7	-5905662.0	1966545.7	4.1	4.4	5.3
8009	WIPPOLDER	3923429.9	299866.1	5003013.3	13.3	13.1	15.2	3923397.4	299869.4	5002975.5	8.5	10.1	6.9
8010	ZIMMERWALD	4331312.7	567499.7	4633118.9	7.9	10.9	11.5	4331307.0	567490.8	4633108.3	5.7	8.3	5.4
8011	MALVERN	3920186.9	-134806.7	5012776.2	12.8	16.5	15.5	3920153.5	-134804.5	5012734.8	8.9	14.3	6.9
8015	HAUTE PROVENCE	4578328.1	457945.6	4403204.8	6.4	10.7	10.2	4578322.1	457936.5	4403195.3	4.2	8.0	4.4
8019	NICE	4579469.1	586582.7	4386428.4	6.3	10.6	10.1	4579463.2	586573.5	4386419.2	4.1	7.9	4.3
8030	MEUDON	4205629.1	163695.4	4776550.9	9.0	12.3	11.8	4205626.9	163683.4	4776540.6	6.5	9.7	5.8
9001	ORGAN PASS	-1535755.1	-5167026.6	3401047.1	4.6	3.9	3.8	-1535750.7	-5167014.4	3401039.4	4.2	2.8	2.7
9002	OLIFANTSFONTEIN	5056115.1	2716514.0	-2775782.9	4.2	3.6	5.3	5056108.4	2716508.7	-2775768.8	3.0	3.0	4.2
9004	SAN FERNANDO	5105589.8	-555269.7	3769680.6	6.3	12.9	8.5	5105581.5	-555271.5	3769676.0	3.4	10.0	4.0
9005	TOKYO	-3946751.4	3366303.2	3698830.3	11.2	10.3	9.8	-3946730.5	3366286.1	3698822.9	9.2	9.0	7.5
9006	NAINI TAL	1018153.3	5471119.3	3109622.2	14.2	10.9	9.6	1018164.5	5471108.7	3109625.6	12.4	5.5	6.0
9007	AREQUIPA	1942762.4	-5804101.6	-1796905.8	2.8	4.0	5.3	1942760.9	-5804088.2	-1796900.9	2.5	2.9	4.4
9008	SHIRAZ	3376872.6	4403990.0	3136250.1	8.1	10.3	9.5	3376875.2	4403976.2	3136257.3	6.8	6.1	6.1
9009	CURACAO	2251613.5	-5816933.6	1327169.7	2.8	3.5	3.8	2251810.7	-5816917.6	1327163.4	2.4	2.1	3.4
9010	JUPITER	976276.2	-5601418.8	2880244.0	2.5	3.3	3.3	976276.2	-5601402.2	2880234.5	2.1	1.8	2.3
9011	VILLA DOLORES	2280578.9	-4914584.8	-3355398.8	2.7	3.6	5.3	2280575.3	-4914580.2	-3355383.7	2.4	2.7	3.7
9012	MAUI	-5466088.5	-2404310.5	2242188.7	4.5	3.4	3.9	-5466067.8	-2404312.7	2242180.4	3.0	2.9	3.3
9021	MOUNT HOPKINS	-1936799.1	-5077719.4	3331926.1	7.3	6.8	6.4	-1936789.3	-5077714.7	3331922.7	7.1	5.3	5.3
9028	ADDIS ABABA	4903727.7	3965208.6	963853.2	2.8	2.9	3.4	4903726.6	3965206.3	963859.6	2.1	2.1	2.9
9029	NATAL	5186459.3	-3653074.6	-654317.9	3.4	2.9	3.2	5186441.4	-3653071.9	-654314.1	2.1	2.2	2.7
9031	CONCORDIA R*DAVIA	1693795.5	-4112354.3	-4556644.1	8.4	9.4	14.3	1693797.3	-4112353.1	-4556622.0	8.3	8.8	11.2
9051	ATHENS	4606866.7	2029708.0	3903567.4	6.0	12.6	8.9	4606861.5	2029692.2	3903562.2	4.2	10.3	4.4
9091	DIONYSOS	4595164.1	2039433.4	3912675.8	6.0	12.6	8.9	4595158.9	2039417.6	3912670.6	4.2	10.3	4.4
9424	COLD LAKE	-1264834.5	-3466912.6	5185449.2	5.2	6.5	7.7	-1264831.9	-3466915.4	5185450.9	4.7	5.5	4.3
9425	EDWARDS AFB	-2450022.2	-4624438.2	3635041.1	3.1	3.2	3.8	-2450012.7	-4624431.6	3635036.6	2.6	2.2	2.4
9426	HARESTUA	3121262.6	592607.0	5512720.9	9.6	11.4	15.5	3121261.3	592605.7	5512723.0	8.6	9.4	5.8
9427	JOHNSTON ISLAND	-6007458.1	-1111834.2	1825730.0	10.9	20.6	8.8	-6007428.7	-1111852.5	1825733.9	8.9	19.8	8.6
9431	RIGA	3183691.2	1421439.3	5322819.8	13.1	11.7	14.7	3183897.6	1421426.7	5322814.7	12.3	9.4	7.0
9432	UZHGOROD	3907423.8	1602394.2	4763932.7	10.2	12.6	13.7	3907419.2	1602378.6	4763922.1	7.9	10.4	5.9

6. Acknowledgment

This investigation was partially sponsored through NASA Grant No. NGL 36-008-093. Some free computer time was provided by The Ohio State University Computer Center.

Grateful acknowledgment is given to the organizations mentioned in the introduction for supplying the observational data, the basic ingredients of this work, and other information always without reservations or delay.

The author wishes also to acknowledge his appreciation to M. Kumar, J.P. Reilly, N.K. Saxena and T. Soler for their part in handling the computer work, and for other assistance, many times on call beyond duty.

7. References

ANDERLE, R.J. 1973. Transformation of Terrestrial Survey Data to Doppler Satellite Datum. *J.geophys.Res.* (in press).

BLAHA, G. 1971. Inner Adjustment Constraints with Emphasis on Range Observations. *Reports of the Department of Geodetic Science* 148,The Ohio State University,Columbus Ohio.

GAPOSCHKIN, E.M., VEIS, G. & LATIMER, J. 1973. Smithsonian Institution Standard Earth III Coordinates. *First International Symposium, The Use of Artificial Satellites for Geodesy and Geodynamics.* Athens.

HEISKANEN, W.A. & MORITZ, H. 1967. *Physical Geodesy.* Freeman,San Fransisco.

KUMAR, M. 1972. Coordinate Transformation by Minimizing Correlations Between Parameters. *Reports of the Department of Geodetic Science* 184,The Ohio State University,Columbus Ohio.

LERCH, F.J. ET AL. 1972. Gravitational Field Models for the Earth. *International Symposium on Earth Gravity Models and Related Problems.* St. Louis Missouri.

MARSH, J.G., DOUGLAS, B.C. & KLOSKO, S.M. 1973. A Global Station Co-ordinate Solution Based Upon Camera and Laser Data - GSFC 1973. *First International Symposium,The Use of Artificial Satellites for Geodesy and Geodynamics.* Athens.

MARTIN, C.F. & VAN FLANDERN, T.C. 1970. Secular Changes in the Lunar Ephemeris. *Science* 168,246-247.

MUELLER, I.I. & WHITING, M.C. 1972. Free Adjustment of a Global Satellite Network (Solution MPS-7). *Reports of the Department of Geodetic Science* 188,The Ohio State University,Columbus Ohio.

MUELLER, I.I., KUMAR, M., REILLY, J.P. & SAXENA, N. 1973a. Free Geometric Adjustment of the DOC/DOD Cooperative Worldwide Geodetic Satellite (BC-4) Network. *Reports of the Department of Geodetic Science* 193,The Ohio State University,Columbus Ohio.

MUELLER, I.I., KUMAR, M & SOLER, T. 1973b. Free Geometric Adjustment of the SECOR Equatorial Network. *Reports of the Department of Geodetic Science* 195,The Ohio State University, Columbus Ohio.

MUELLER, I.I. & KUMAR, M. 1973c. Geometric Adjustment of the South American Satellite Densification (PC-1000) Network. *Reports of the Department of Geodetic Science* 196,The Ohio State University,Columbus Ohio.

MUELLER, I.I., KUMAR, M., REILLY, J.P., SAXENA, N. & SOLER, T. 1973d. Global Satellite Triangulation and Trilateration for the National Geodetic Satellite Program. *Reports of the Department of Geodetic Science* 199,The Ohio State University,Columbus Ohio.

RAPP, R.H. 1973. Comparison of Least Squares and Collocation Estimated Potential Coefficients. *Reports of the Department of Geodetic Science* 200,The Ohio State University,Columbus Ohio.

8. Discussion

MELCHIOR: Can you tell me where the BIH zero meridian is, and where CIO is?

MUELLER: Theoretically, the BIH zero meridian and CIO should be exactly those of WN14, for they were enforced in this solution.

MELCHIOR: The NWL solution has also been adjusted to that.

MUELLER: These numbers (transformation parameters) are based on the published co-ordinates and there is no agreement. We have done a lot of thinking since this thing was noticed last June and there is no easy explanation. In the dynamic solution, due to the fact that some of the harmonic coefficients are enforced to be zero, some biasing can happen to the co-ordinate systems. I hope that next summer we can have a conference on the topic to resolve this problem.

BOMFORD: A variety of co-ordinates are being produced for stations on the world network. In Europe, no co-ordinate system has yet been adopted because every four years at the IAG more information is produced which people think should be included. I ask our colleagues from the United States if WN14, which I think is an excellent solution, is likely to be adopted in any formal way? Do we wait till we go to Grenoble in 1975, by which time there is likely to be some more information? What is likely to happen?

MUELLER: I think this is a political question. I really cannot answer this at all. We have to keep producing improved solutions and let someone else decide on which of the systems should be used. A scientist always *uses* the best current solution and not an earlier *adopted* one. My suggestion is : Don't wait for an international body to adopt a solution. A user should decide on which set suits his needs and then determine the relations between this system and all other available systems.

RAPP, R.H.
Department of Geodetic Science
The Ohio State University
Columbus Ohio 43210
United States of America

Proc.Symposium on Earth's Gravitational Field & Secular Variations in Position (1973),554-558.

ADJUSTED PARAMETERS OF A MEAN EARTH ELLIPSOID

ABSTRACT

Independent estimates of **a**, J_2, kM_E (of the solid Earth), R_o (scale factor for lengths), γ_e (equatorial gravity) and a fixed ω are used in a weighted least squares adjustment to determine adjusted values for the variable parameters assuming a rotational bi-axial equipotential ellipsoid as the figure of reference. The adjusted values are:

$kM_E = (3.986\ 003\ 4 \pm 0.000\ 002\ 3) \times 10^{14}\ m^3 sec^{-2}$;

$\gamma_e = 978\ 031.69 \pm 0.77$ mgal;

$f = 1/(298.256\ 36 \pm 0.001\ 47)$;

$R_o = 6\ 363\ 674.98 \pm 2.50$ m;

$a = 6\ 378\ 139.0 \pm 2.51$ m; and

W_o (the geoid potential) = 6 263 681.62 kgal m.

1. Introduction

The estimation of the parameters of a mean Earth ellipsoid is one of the important goals of geodetic work. This paper is written to briefly summarize the results found recently for mean Earth ellipsoid parameters using currently available data. A more detailed paper is currently in preparation.

2. Dynamic Ellipsoid Parameters

We define the ellipsoid of interest to be an equipotential bi-axial ellipsoid. We consider the following quantities related to this ellipsoid:

ω, the rotational velocity of the ellipsoid. We adopt the value for ω as used in the Geodetic Reference System 1967: $\omega = 0.729\ 211\ 514\ 67 \times 10^{-4}$ (IAG 1971). This value is considered fixed.

kM_E, the geocentric gravitational constant of the Earth excluding the atmosphere. A current estimate of kM including the atmosphere is $kM_{E+A} = 3.986\ 008\ 0 \times 10^{14} m^3 sec^{-2}$ (ESPOSITO & WONG 1972). Discussions with Esposito indicate that a reasonable standard deviation for this estimate is $\pm 0.000\ 002\ 5 \times 10^{14} m^3 sec^{-2}$. To determine kM_E we subtract the mass of the atmosphere given by OLCZAK (1970) as $kM_A = 0.000\ 003\ 4 \times 10^{14} m^3 sec^{-2}$, yielding $kM_E = (3.986\ 004\ 6 \pm 0.000\ 002\ 5) \times 10^{14} m^3 sec^{-2}$ for the value to be used in this paper.

γ_e, equatorial gravity. Given a set of gravity anomalies referred to an arbitrary gravity formula, a new gravity formula (a γ_e, and a flattening) can be derived by least squares techniques (HEISKANEN & VENING MEINESZ 1958,p.76). Using a set of 24,260 1° × 1° mean free air anomalies a best estimate of γ_e was determined to be $978\ 030.9 \pm 1$ mgal where the flattening implied by the gravity formula was fixed at 1/298.256. In determining

this γ_e, all anomalies were given equal weights and a Potsdam correction of -14 mgal (IAG 1971) was used.

f, the flattening. The flattening was not directly estimated. Instead we choose to use a determination of J_2, the second degree zonal potential coefficient, as carried out by WAGNER (1972). The value of J_2 used was $(1082.635 \pm 0.011) \times 10^{-6}$. J_2 can be almost directly related to the flattening using equations given by COOK (1959) or HEISKANEN & MORITZ (1967, p.73).

R_o, the scale factor for lengths is defined to be (BURSA 1969)

$$R_o = kM/W_o \qquad (1),$$

where W_o is the potential on the geoid. If we know the geocentric positions of points on the geoid, we can determine W_o from (IBID)

$$W_o = \frac{kM_E}{r_i}\left(1 + \sum_{\ell=2}^{N}\left(\frac{a}{r_i}\right)^{\ell}\sum_{m=0}^{\ell}\left(\overline{C}_{\ell m}\cos m\lambda + \overline{S}_{\ell m}\sin m\lambda\right)\overline{P}_{\ell m}(\sin\Phi)\right) + \frac{\omega^2 r_i^2}{2}\cos^2\Phi \qquad (2),$$

where: r_i = the geocentric radius to the geoid point;
Φ = the geocentric latitude; and
$\overline{C}_{\ell m}, \overline{S}_{\ell m}$ = fully normalized potential coefficients.

Considering equation 1, we can see that R_o can be estimated (almost) independently of kM. The R_o is not completely independent of kM since the scale of the geocentric radius depends on the kM used in a satellite solution for geocentric station co-ordinates.

In order to estimate R_o we used the recent solution of the SAO Standard Earth III, and the Goddard Earth Model (GEM) 6. Both of these solutions used a $kM_{E+A} = 3.986\,013 \times 10^{14} m^3 sec^{-2}$ for their primary scale determination. Since we have decided to use a $kM_{E+A} = 3.986\,008\,0 \times 10^{14} m^3 sec^{-2}$ as our best estimate, we scaled the station co-ordinates of the SE III and GEM 6 using the $\Delta kM/3kM$ change discussed by KAULA (1967). After this a value of R_o was estimated separately for each solution with a weighted mean value of $R_o = 6\,363\,676.0 \pm 4.0\ m$ being found. The standard deviation assiged to R_o was computed considering the following factors:

- neglect of higher degree potential coefficients,
- errors in the potential coefficients,
- errors in the station co-ordinates,
- consistency of the R_o values from each solution, and
- the error in kM.

a, the equatorial radius may be computed from some or all of the above data. For example, the data needed for computing W_o, can be used to determine an equatorial radius. For this paper, however, we wish to determine an "a" from methods independent of previous data used. Such a method lies within the recent results from the geometrical satellite triangulation networks. In a presentation SCHMID (1972) indicated an equatorial radius from his geometric net to be on the order of 6 378 130 m. MUELLER (1973) gave a result for his geometric analysis only, of 6 378 125.8 m. Consideration of this data leads us to use an equatorial radius estimate of 6 378 128 ± 6 m where the standard deviation is based on accuracy considerations for the WN14 solution as given in (IBID).

3. The Adjustment

At this point we note that we need adopt only four parameters to completely define our mean Earth ellipsoid. If we use such a procedure, however, we will be forced to choose which of the above parameters are most reliable. An alternative procedure is to use all our data estimates and carry out a weighted least squares adjustment.

To formulate our adjustment model we first re-write equation 2-61 from (HEISKANEN & MORITZ 1967,p.67) to put it in the form:

$$\frac{1}{R_o} = \frac{W_o}{kM} = \frac{\tan^{-1} e'}{ae} + \frac{1}{3}\frac{\omega^2 a^2}{kM} \qquad (3).$$

We then write (IBID,equation 2-73) in the following form:

$$kM_E = \gamma_e a\, b \left(1 - m - \frac{m}{6}\frac{e'\, q'_0}{q_0}\right)^{-1} \qquad (4)$$

where all terms not defined here may be found in the reference quoted. Equations 3 and 4 were conceptually modified to incorporate J_2 as a shape (or flattening) parameter instead of the first (e) or second (e') eccentricity.

Considering equations 3 and 4 as our basic functional model, a generalized least squares adjustment was carried out. The a priori values and the standard deviations of the parameters kM_E, γ_e, J_2, R_o and **a** were assigned as previously discussed. The adjusted values were then obtained after the adjustment. A summary of the "a priori" values and the adjusted values are given in table 1.

Table 1

Adjustment of Earth Parameters

	A Priori	Adjusted	Units
ω*	7.292 115 146 7	7.292 115 146 7	$\times 10^{-5}$ sec^{-1}
kM_E	3.986 004 6 ±0.000 002 5	3.986 003 4 ±0.000 002 3	$\times 10^{14}$ m^{3}sec^{-2}
γ_e	978 030.9 ± 1.0	978 031.69 ± 0.77	mgal
J_2	1082.635 ± 0.011	1082.635 ± 0.011	$\times 10^{-6}$
R_o	6 376 676.0 ± 4.0	6 363 674.98 ± 2.50	m
a	6 378 128.0 ± 6.0	6 378 139.00 ± 2.51	m
kM^+_{E+A}	3.986 008 0	3.986 006 8	10^{14} m^{3}sec^{-2}
$W^+_o = \frac{kM_E}{R_o}$	6 263 682.5	6 263 681.62	kgal m
1/f +	298.257 18	298.256 36 ±0.001 47	

+ Derived Quantities * Fixed

The adjusted values given in table 1 are best estimates on the basis of the data available. As these change, so will the adjusted values. For example, if we let our a priori estimate of a have a standard deviation of 200 m, the adjusted value of "a" will be increased by 2.34 m.

4. Conclusions

The main results given in this paper are the numerical values given in table 1. They represent the results obtained by utilizing more data than the minimum needed to define an equipotential ellipsoid. The a priori values are based on current estimates of the parameters with, hopefully, realistic standard deviations.

The adjustment model incorporating R_o was chosen preferable to one incorporating W_o because W_o is strongly dependent on kM and thus estimates of W_o and kM would be correlated. The use of R_o eliminates most of the correlation although a small amount remains through the dependence of the magnitude of the geocentric radius on the adopted value of kM on the satellite solution. The potential correlation between R_o and kM was considered by performing adjustments where the correlation coefficient between R_o and kM was varied between 0.1 and 0.9. The effect on the results was less than 1 part in 10^7 and considered negligible.

The technique described in this paper allows us to use estimates of all the parameters defining a mean Earth ellipsoid and thus does not force us into the position of choosing what might be considered by some to be the most reliable parameters.

5. Acknowledgment

The computer time used in this study was provided by the Instruction and Research Computer Center of The Ohio State University.

Mr. D.P. Hajela carried out the necessary derivations for the adjustment procedures described here and prepared the necessary computer programs for carrying out the adjustment.

6. References

BURSA, M. 1969. Potential of the Geoidal Surface, the Scale Factor for Lengths and Earth's Figure Parameters from Satellite Observations. *Studia geophys. et geodet.* 13,337-358.

ESPOSITO, P.B. & WONG, S.K. 1972. Geocentric Gravitational Constant Determined from Mariner 9 Radio Tracking Data. *International Symposium on Earth Gravity Models & Related Problems*, St. Louis Mo.

IAG 1971. *Geodetic Reference System 1967.* Special Publication,International Association of Geodesy, Paris.

HAJELA, D.P. 1973. *Earth Model Parameter Adjustment Procedure.* (unpubl.) Department of Geodetic Science,The Ohio State University,Columbus Ohio.

HEISKANEN, W.A. & MORITZ, H. 1967. *Physical Geodesy.* Freeman,San Fransisco.

HEISKANEN, W.A. & VENING MEINESZ, F.A. 1958. *The Earth and its Gravity Field.* McGraw Hill,New York.

KAULA, W.M. 1967. Comparison and Combination of Satellites with Other Results for Geodetic Parameters. In (VEIS, G. ed.) *The Use of Artificial Satellites for Geodesy, Vol.II.* National Technical University,Athens.

MUELLER, I.I. 1973. Earth Parameters from Global Satellite Triangulation and Trilateration. In *Proceedings of Symposium on Earth's Gravitational Field & Secular Variations in Position*, University of New South Wales,Kensington NSW.

OLCZAK, T. 1970. The Earth Ellipsoid and Some Physical Constants Associated with It. *Acta Geophysica Polonica* XVIII(3-4) (Transl. Defence Mapping Agency Aerospace Center TC-1729,1971)

SCHMID, H. 1972. Presentation to 5th Symposium on Mathematical Geodesy (2nd Hotine Symp.),Florence.

WAGNER, C.A. 1972. Earth Zonal Harmonics from Rapid Numerical Analysis of Long Satellite Arcs. *Doc. X*-553-72-341, Goddard Space Flight Center, Greenbelt Md.

GRAFAREND, E.W.
Institut für Theoretische Geodäsie
Universität Bonn
Bonn
Federal Republic of Germany

Proc. Symposium on Earth's Gravitational Field & Secular Variations in Position (1973), 559.

VARIATIONAL PRINCIPLES AND THE ELLIPSOIDAL DATUM

ABSTRACT

Variational principles for the best fitting of a reference figure, for instance an ellipsoid, relative to a planetary figure are analysed in respect of their sensitivity. General orthonormal series solutions are presented for global criteria. Spectra of four difference norms (Euclidian distance, gradient distance, curvature distances) of a geoidal with respect to a rotational symmetric ellipsoidal surface are given and physically interpreted. Relative to a spherical integration surface, the principal semi-axis of a rotational ellipsoid is due to 6,378,132 m, ..., 120 m, ... , 140 m respectively for the Euclidian distance, the gradient distances and the invariant and the invariant curvature distances; its flattening 1/298.2553, ... .2553, ... .2571, ... .2448, ... .2494 respectively.